★

WORLD SALT SYMPOSIUM
June 19-21, 2018 Park City UT, USA

College of Industrial Technology
Nihon University

Enhanced $CaMg(CO_3)_2$ Production by CO_2 Microbubble Injection into Concentrated brine

Masakazu MATSUMOTO [1], **Koji MASAOKA** [2], **Yuko TSUCHIYA** [1], **Yoshinari WADA** [1], **Toshihiko HIAKI** [1], **Kaoru ONOE** [3]

[1] College of Industrial Technology, Nihon University
[2] Research Institute of Salt and Sea Water Science
[3] Faculty of Engineering, Chiba Institute of Technology

How to generate microbubbles?

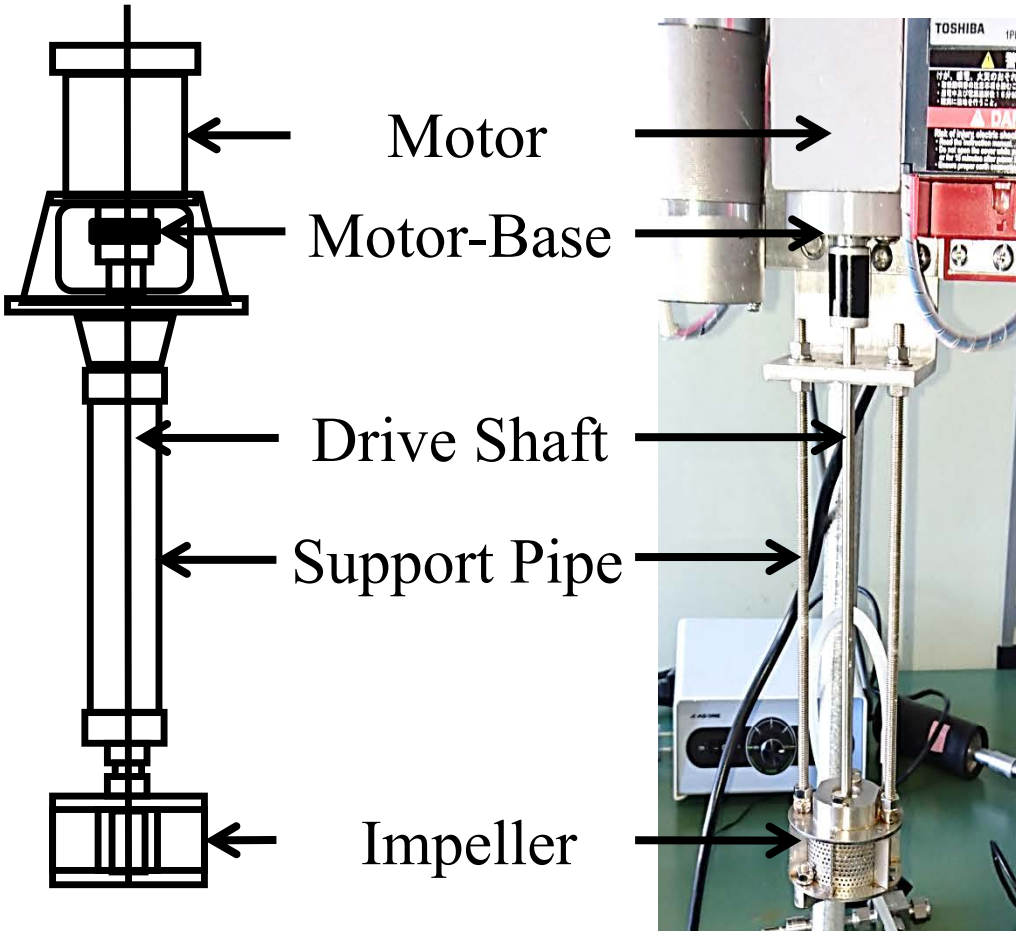

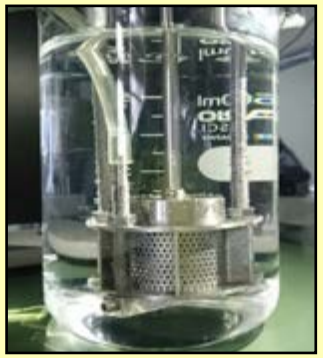

Without microbubbles

Supplying microbubbles

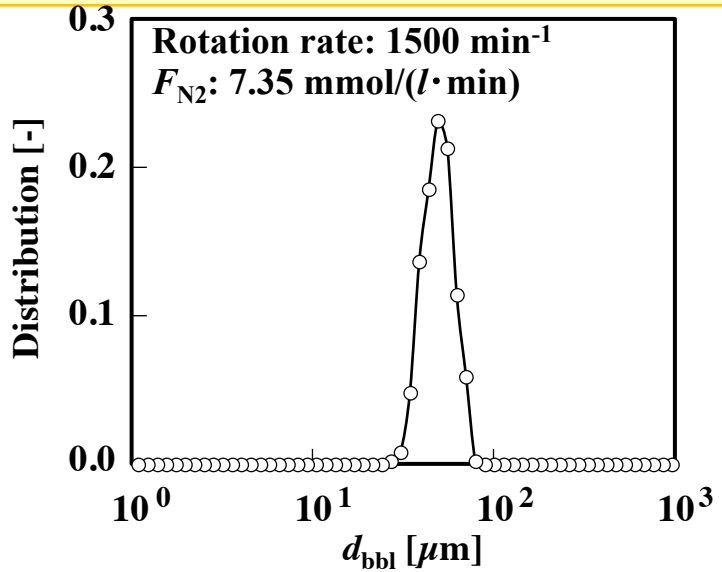

○ Microbubbles are generated using a self-supporting bubble generator by the shear of the impeller and a negative pressure owing to high-rotation.

➡ The average bubble diameter can be varied by controlling the gas flow rate and rotation rate .

Features of minimizing bubble formation

Increase in the gas-liquid interfacial area	Increase in the average residence time of bubbles	Occurrence of Interactions at the gas-liquid interface
Acceleration of mass transfer and gas absorption	Increase of mass transfer rate Improvement of bubble dispersibility	Change in interfacial potential Increase of interfacial adsorption

Gas-liquid interfacial area

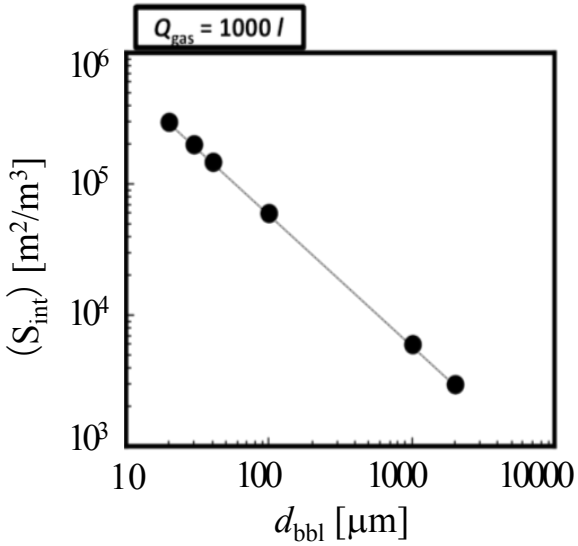

Flotation rate [1)]

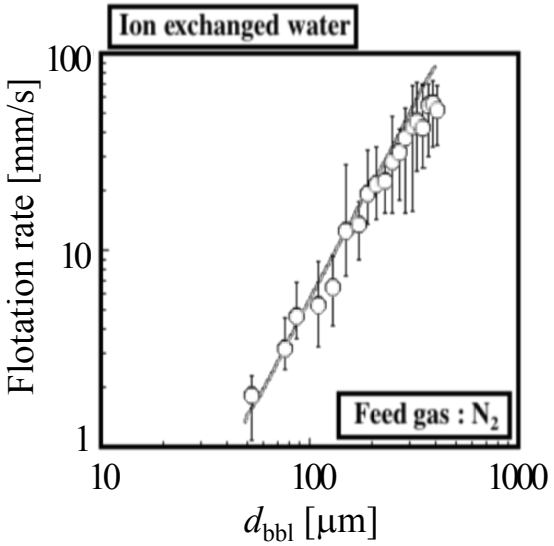

Zeta potential [1)]

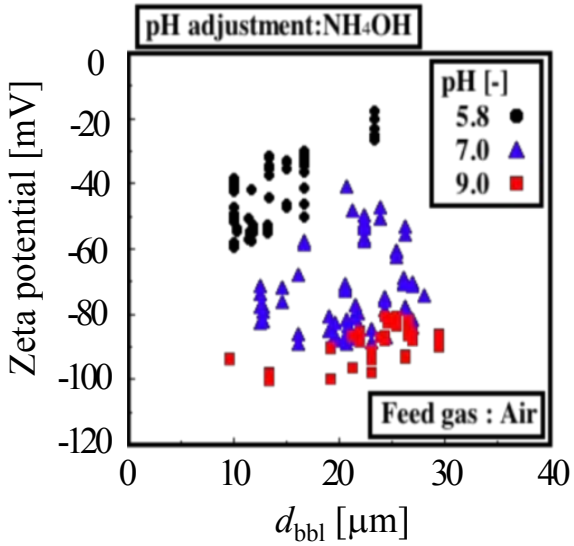

○ The gas-liquid interfacial area increases remarkably by decreasing d_{bbl}.

○ The flotation rate at d_{bbl} of 50 μm is 100 times smaller than that of 500 μm.

○ The zeta potential at d_{bbl} of 10 - 30 μm shows the negative value between -20 and -100 mV.

⇨ ***Microbubbles with the surface potential reside in the liquid phase for a long period of time.***

➡ **Unique mass-transfer patterns and reaction phenomena in the regions around the minute gas-liquid interfaces are expected to occur.**

1) M.Matsumoto *et al.*, *Chem. Eng. Res. Des.*, 88, 1624 (2010)

How build a utilization system for seawater resources based on salt production process ?

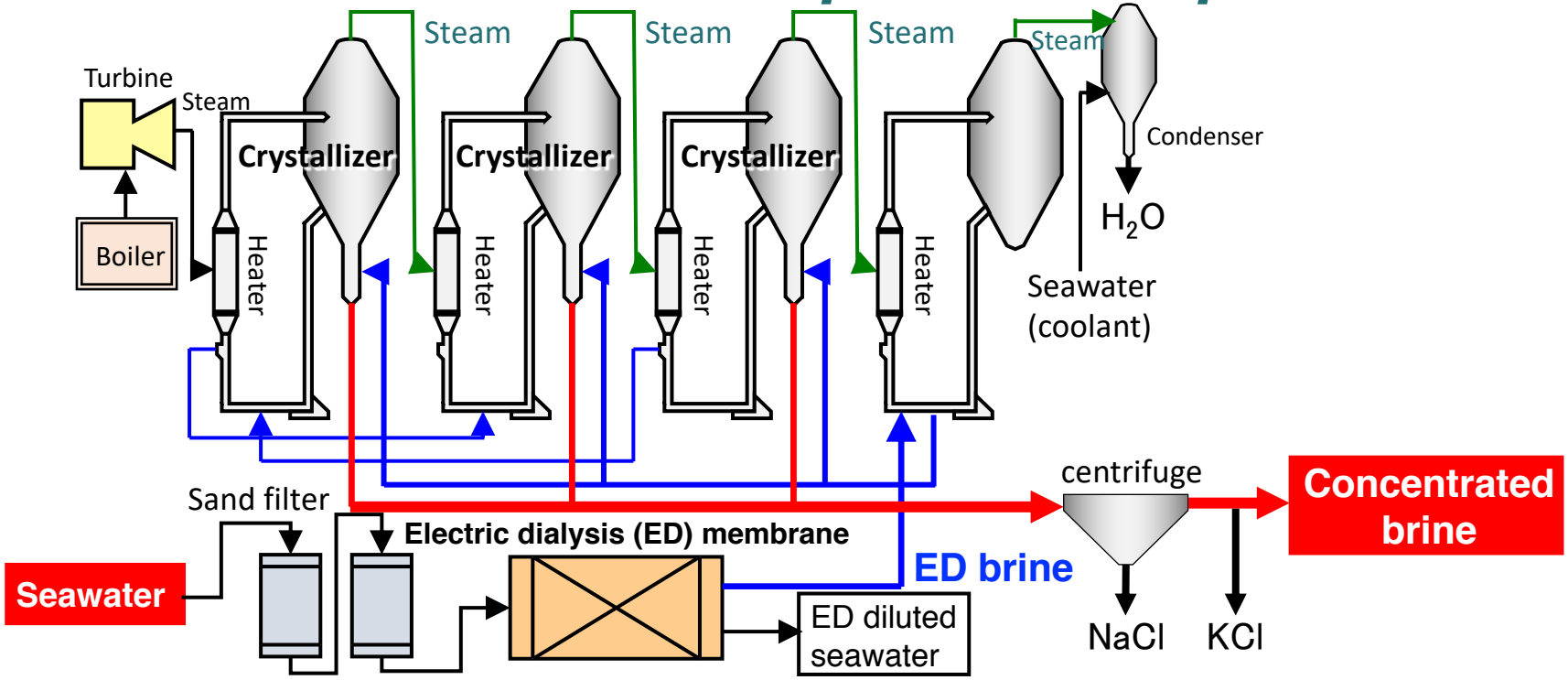

Ion	Concentration [mmol/l][1)] Seawater	Concentrated brine
Ca^{2+}	11	670
Mg^{2+}	54	2140
K^{+}	10	130
Na^{+}	300	840
SO_4^{2-}	27	0
Cl^{-}	530	7100

In Japan, NaCl is manufactured by evaporative crystallization after concentrating seawater through an ED membrane, and the concentrated brine that removed K^{+} by cooling crystallization of KCl is obtained.

A recovery and upgrading method for Ca and Mg from the concentrated brine discharged from salt manufacture in Japan is desired.

1) The Salt Industry Center of Japan(Ed.), "Data book for sea- water science and salt production", 54-91(2006)

How recover Ca and Mg ?

Relation between solution pH and solubility of carbonate and hydroxide

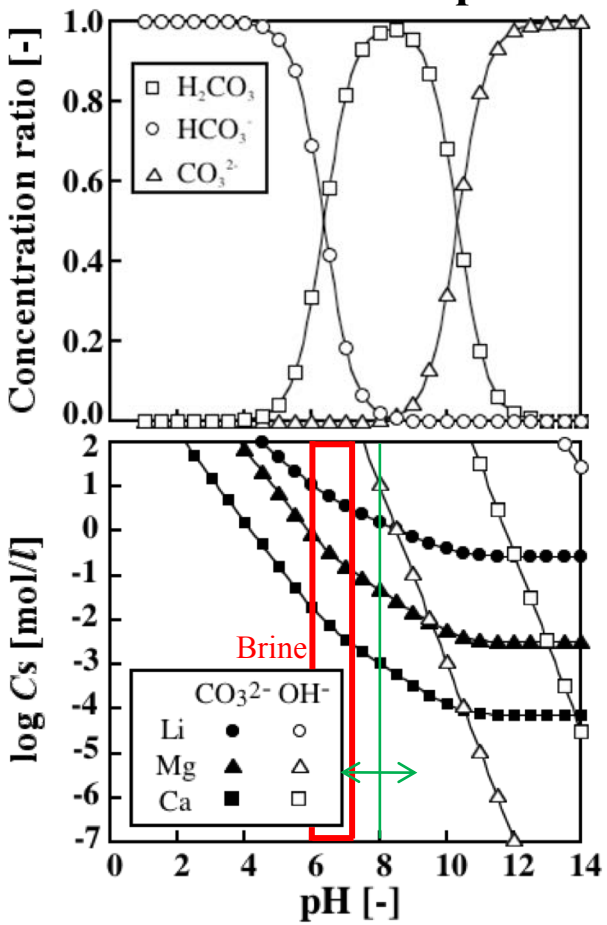

Calculation of solubility

Hydroxide

$$k_{sp}=[Me^{n+}][OH^-]^n = X \quad (1)$$

$$\log[OH^-]=-14+pH \quad (2)$$

$$\log[Me^{n+}]+n\log[OH^-]=\log X \quad (3)$$

$$\log[Me^{n+}]=Y-npH \quad (4)$$

Carbonate

$$\alpha = \frac{[CO_3^{2-}]}{[CO_3^{2-}]+[HCO_3^-]+[H_2CO_3]} \quad (5)$$

$$k_{sp}=[Me^{n+}]^m[CO_3^{2-}] = Cs \times \alpha Cs^m = \alpha Cs^{(m+1)} \quad (6)$$

$$Cs = \sqrt[m+1]{ksp/\alpha} \quad (7)$$

○ The solubility of carbonate is lower than the solubility of hydroxide at pH range below 8.0.

→ The synthesis of carbonate by reactive crystallization between the dissolved Ca^{2+} and Mg^{2+} in the concentrated brine and CO_2 can be considered an effective separation/recovery method.

Crystal properties of $CaMg(CO_3)_2$

$CaMg(CO_3)_2$
Dolomite

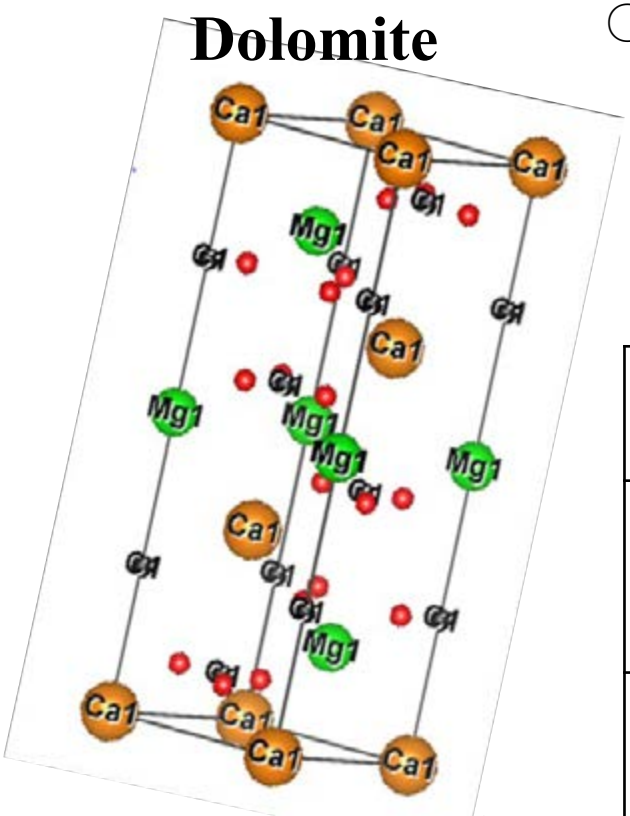

Crystal structure[2)]

- ○ $CaMg(CO_3)_2$ is double salt of $CaCO_3$ and $MgCO_3$.
- ○ $CaMg(CO_3)_2$ has crystal structure derived from that of calcite by ordered replacement Ca^{2+} in calcite by Mg^{2+}.

Crystal structure : **trigonal** Solubility [g/*l*] : **0.26**

Mg/Ca ratio : **1.0**

Classification of dolomite

	Mg/Ca ratio	Particle size [μm]	Usage
Natural dolomite	0.3 - 0.5	2000～	Filler Fireproof material Fertilizer
Synthesized dolomite	1.0	～10	Food additives Drug additives Adsorbent

⇨ To improve the functionality of the crystal for better $CaMg(CO_3)_2$ utilization, it is essential to gain access to Mg/Ca ratio of 1.0 and decrease particle size in the crystallization process.

2) Pilati.T, Demartin.F, Gramaccioli.C.M., Acta Crystallographica Section B, 54, pp.515 - 523 (1998)

How to obtain $CaMg(CO_3)_2$ with Mg/Ca ratio of 1.0 ?

Previous study about Mg/Ca ratio of $CaMg(CO_3)_2$

Generation field of carbonates[3)]

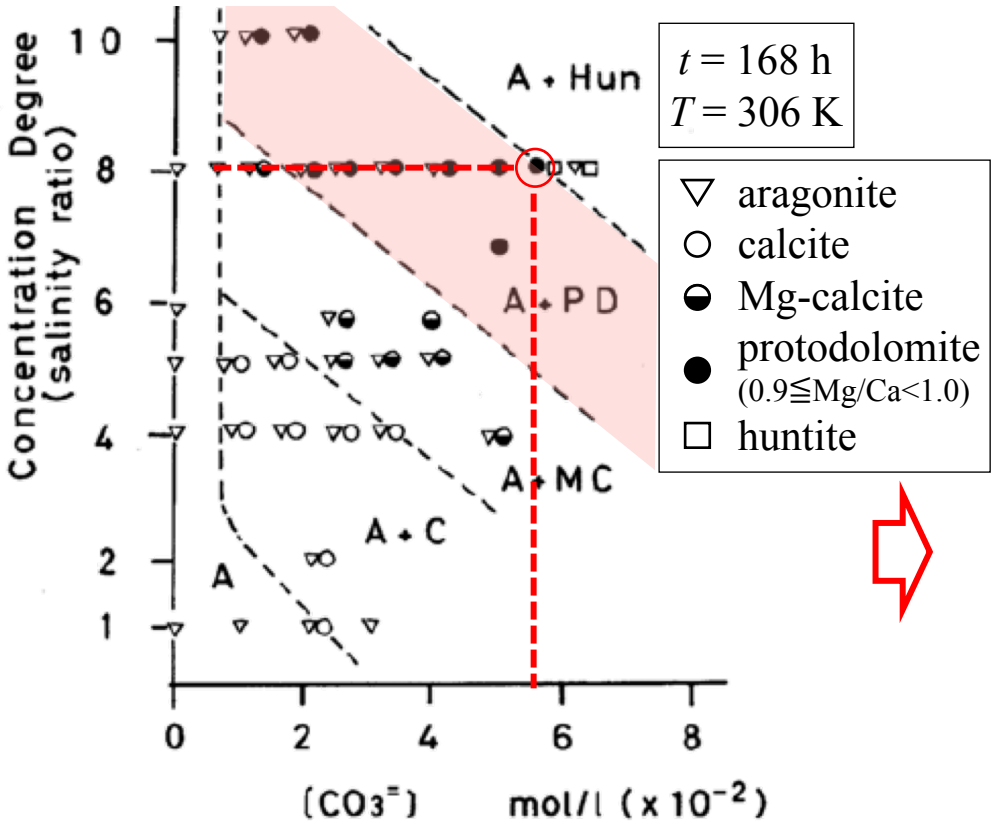

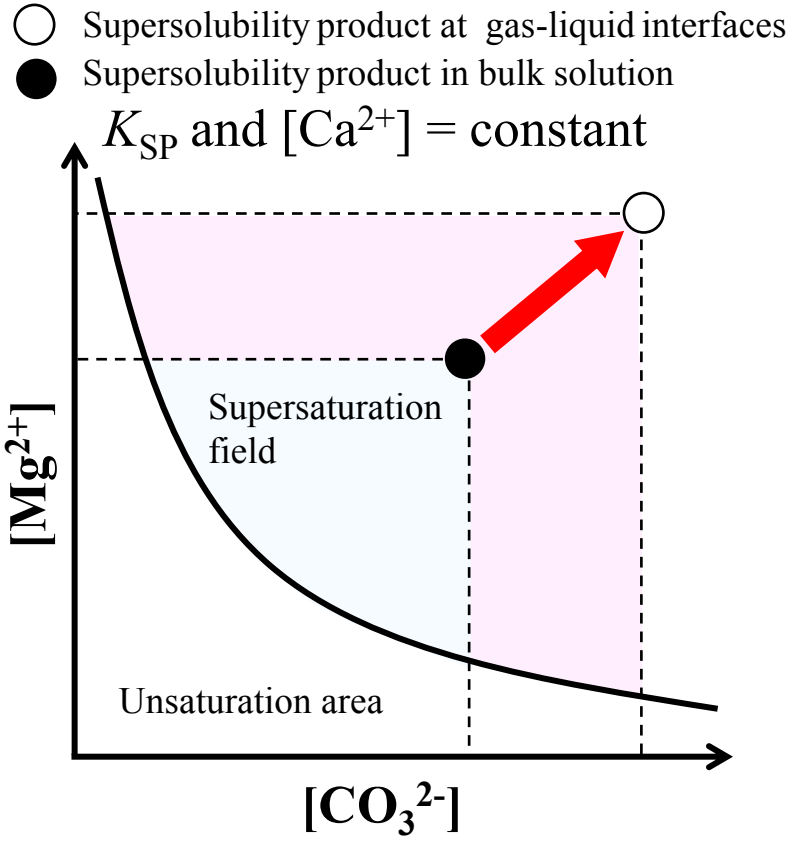

○ Protodolomite was crystallized by adding Na_2CO_3 solution to concentrated seawater.

○ Mg/Ca ratio increased with an increase in the CO_3^{2-} concentration and concentration degree of seawater.

⇨ High concentrations of Ca^{2+}, Mg^{2+} and CO_3^{2-} are necessary for the synthesis of $CaMg(CO_3)_2$ with Mg/Ca ratio of 1.0.

3) T.Oomori, Y.Kitano, *Geochemical Journal,* 21, 59 (1987)

Effects of minimizing bubble diameter on reactive crystallization of $CaMg(CO_3)_2$

Zeta-potential of microbubbles

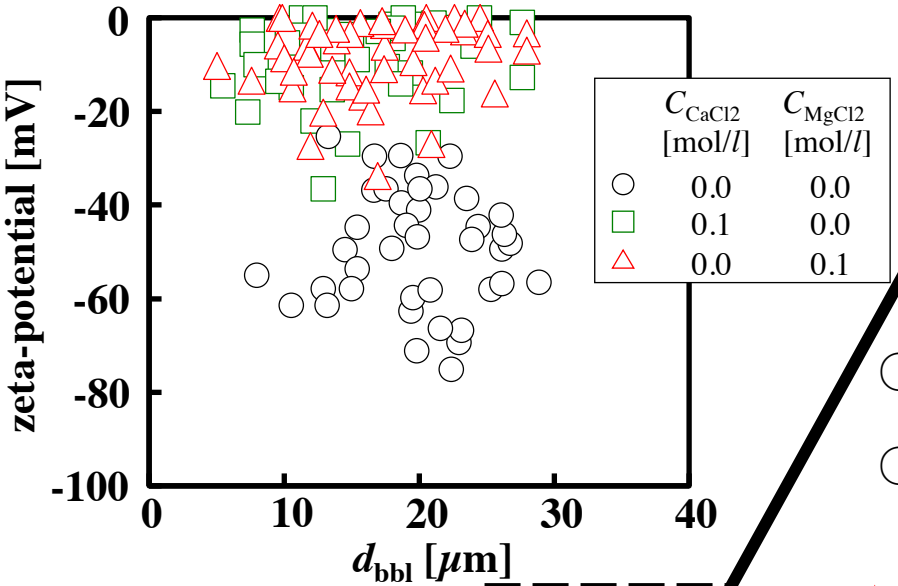

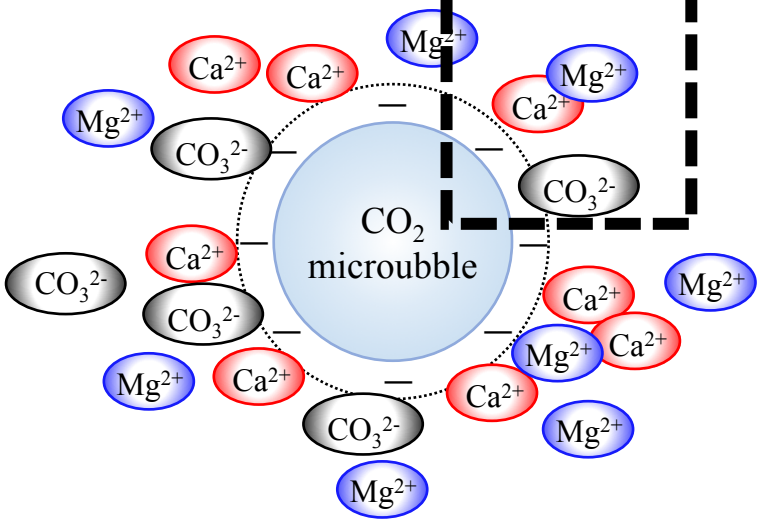

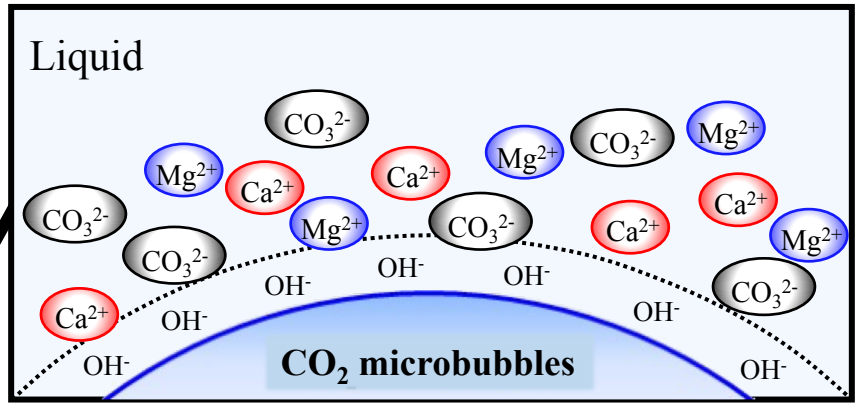

- Ca^{2+} and Mg^{2+} accumulate because of the negative charge on the microbubble surface.
- The CO_3^{2-} concentration becomes higher due to the acceleration of the CO_2 mass transfer.

The generation of crystal nuclei is faster and the fine particles of $CaMg(CO_3)_2$ with a high Mg/Ca ratio is crystallized.

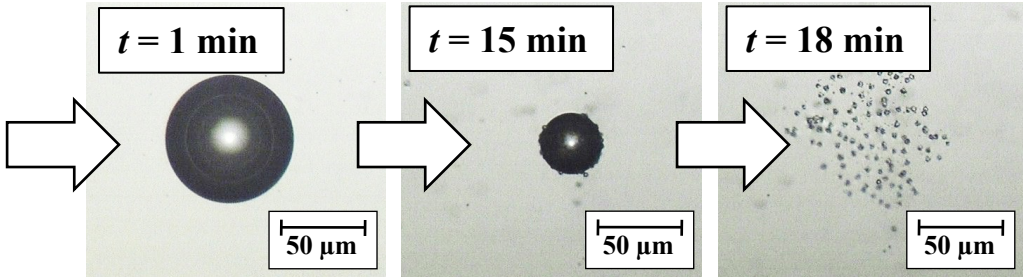

The gas-liquid interfaces of the microbubbles can be utilized as new reactive crystallization fields.

Outline of this study

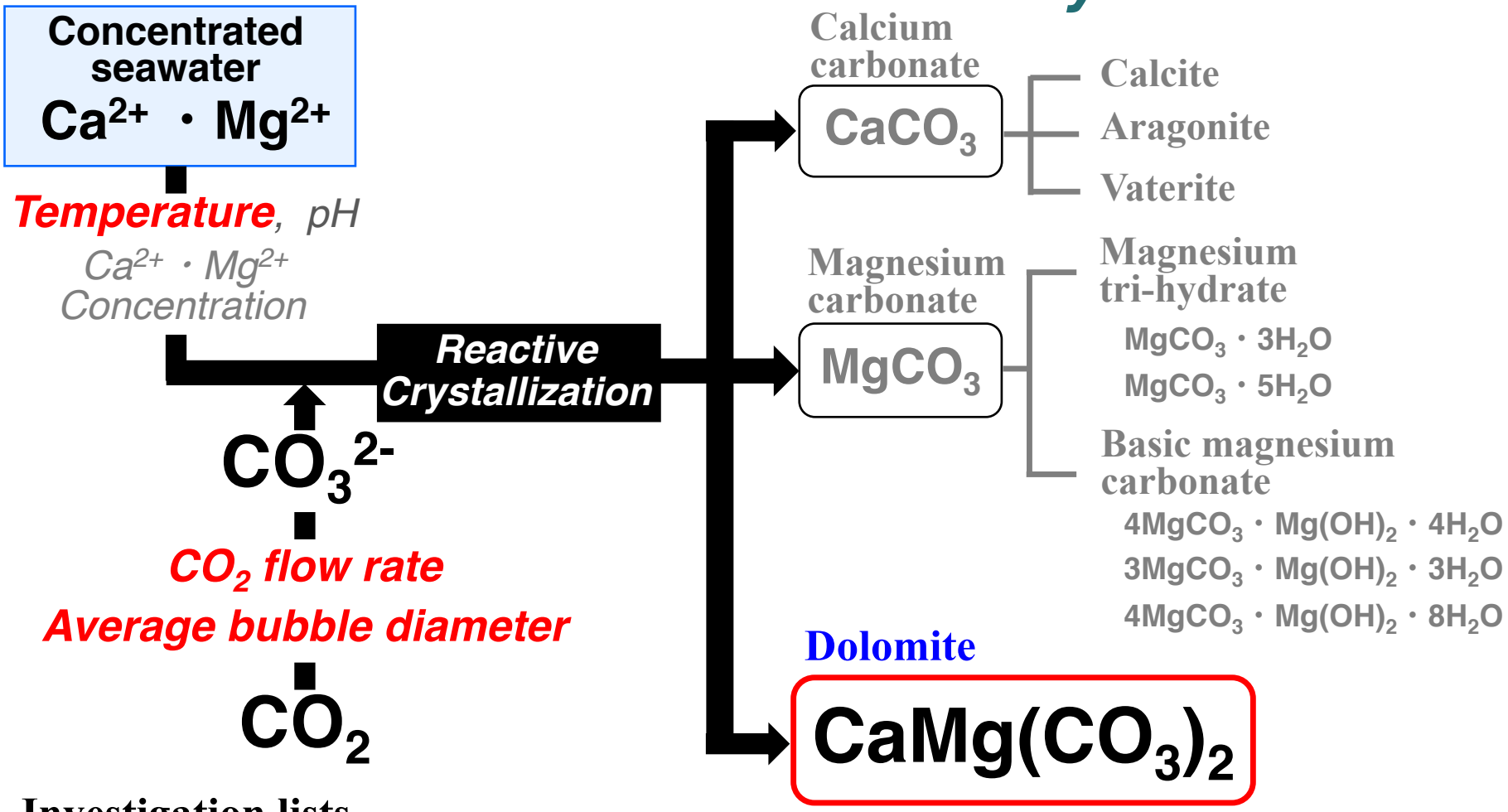

Investigation lists

○ The effects of minimizing the bubble diameter on the reactive crystallization of $CaMg(CO_3)_2$.

○ The effects of CO_2 flow rate and reaction temperature on the crystal properties of $CaMg(CO_3)_2$ during reactive crystallization with CO_2 microbubble injection.

Semi-batch type crystallization apparatus

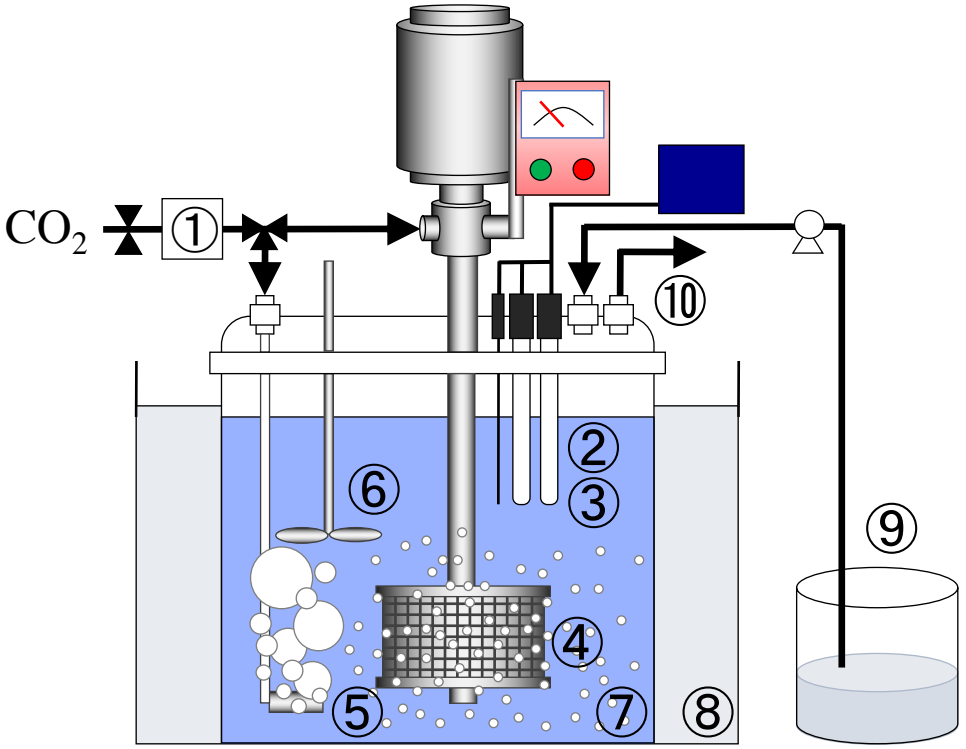

① Gas flow controller
② pH/EC meter
③ Thermocouple
④ Self-supporting bubble generator
⑤ Dispersing-type bubble generator
⑥ Propeller-type mixer with four blades
⑦ Crystallization vessel
⑧ Thermostated bath
⑨ Feed tank
⑩ Gas exit

Bubble generator	Self-supporting	Dispersing-type
Average bubble diameter (d_{bbl}) [μm]	40	200 – 2000
Rotation rate [min^{-1}]	1500	1000
CO_2 flow rate (F_{CO2}) [mmol/(l ・ min)]	1.49 – 23.8	5.96 – 23.8

Experimental conditions

Concentrated brine*		
Concentrations of major ions [mmol/*l*]		
Ca^{2+} ion	0.67	
Mg^{2+} ion	2.1	
Na^{+} ion	0.84	
Cl^{-} ion	7.1	
Volume [m*l*]	300	
Bubble generator	Self-supporting	Dispersing-type
Average bubble diameter (d_{bbl}) [μm]	40	200 – 2000
CO_2 flow rate (F_{CO2}) [mmol/(*l* · min)]	1.49 – 23.8	5.96 – 23.8
Reaction time (t_r) [min]	0 - 120	
Reaction temperature (T_r) [K]	293 – 313	
Reaction pH [-]	6.8	
pH adjustment	NaOH aqueous solution	

*The concentrated brine discharged from salt manufacture was used.

How is Mg/Ca ratio of $CaMg(CO_3)_2$ determined?

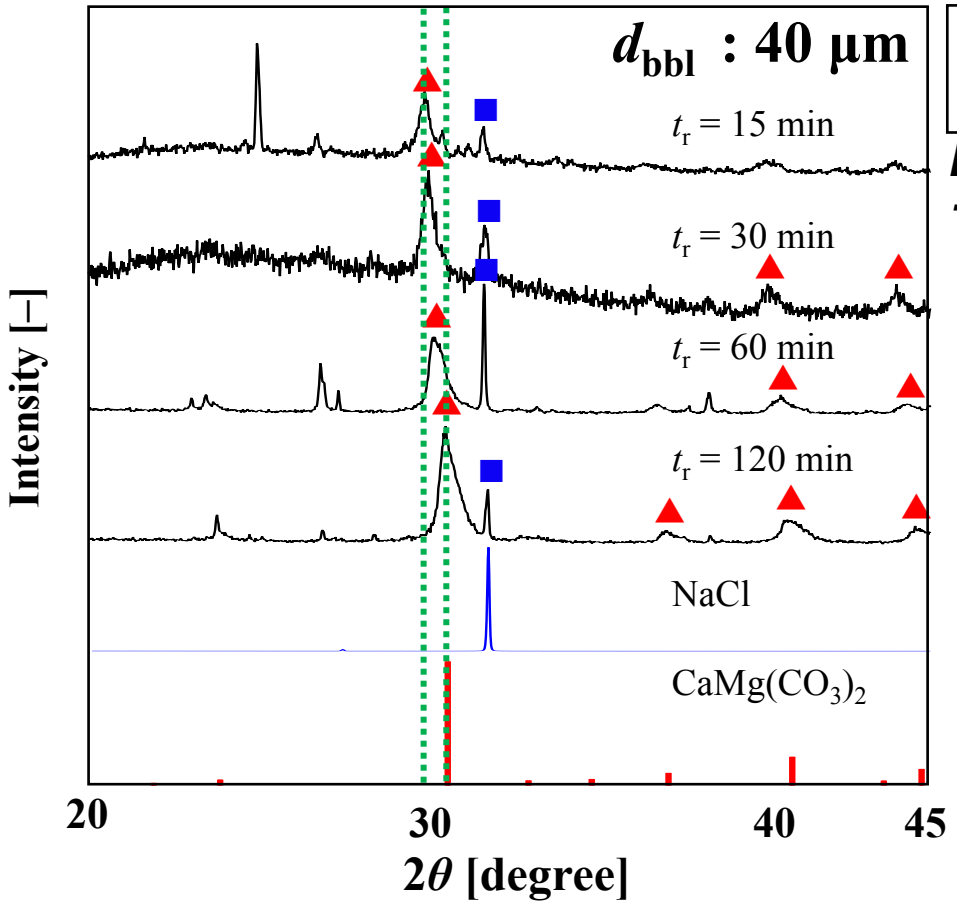

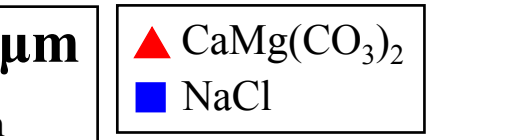

F_{CO2}: 11.9 mmol/(*l*·min)

T_r : 298 K

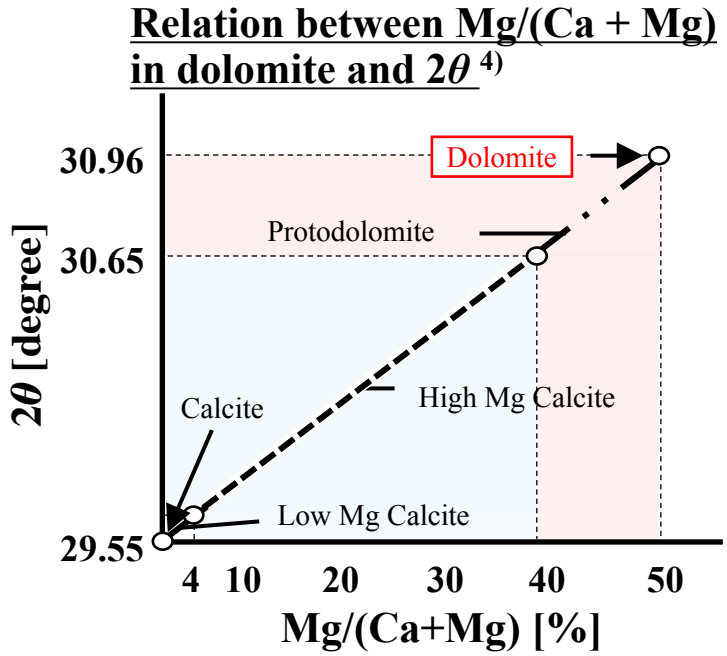

○ XRD peak of calcite ($2\theta = 29.4^\circ$) shifted to $CaMg(CO_3)_2$ ($2\theta = 30.7^\circ$) with an increase in Mg/Ca ratio.

→ Mg/Ca ratio of $CaMg(CO_3)_2$ was estimated from the amount of peak shift from calcite to $CaMg(CO_3)_2$.

4) H.Michishio, *et. al., Research reports of Kochi University Natural science*, 32 , 327 (1983)

Effects of minimizing bubble diameter on time change in the produced weight

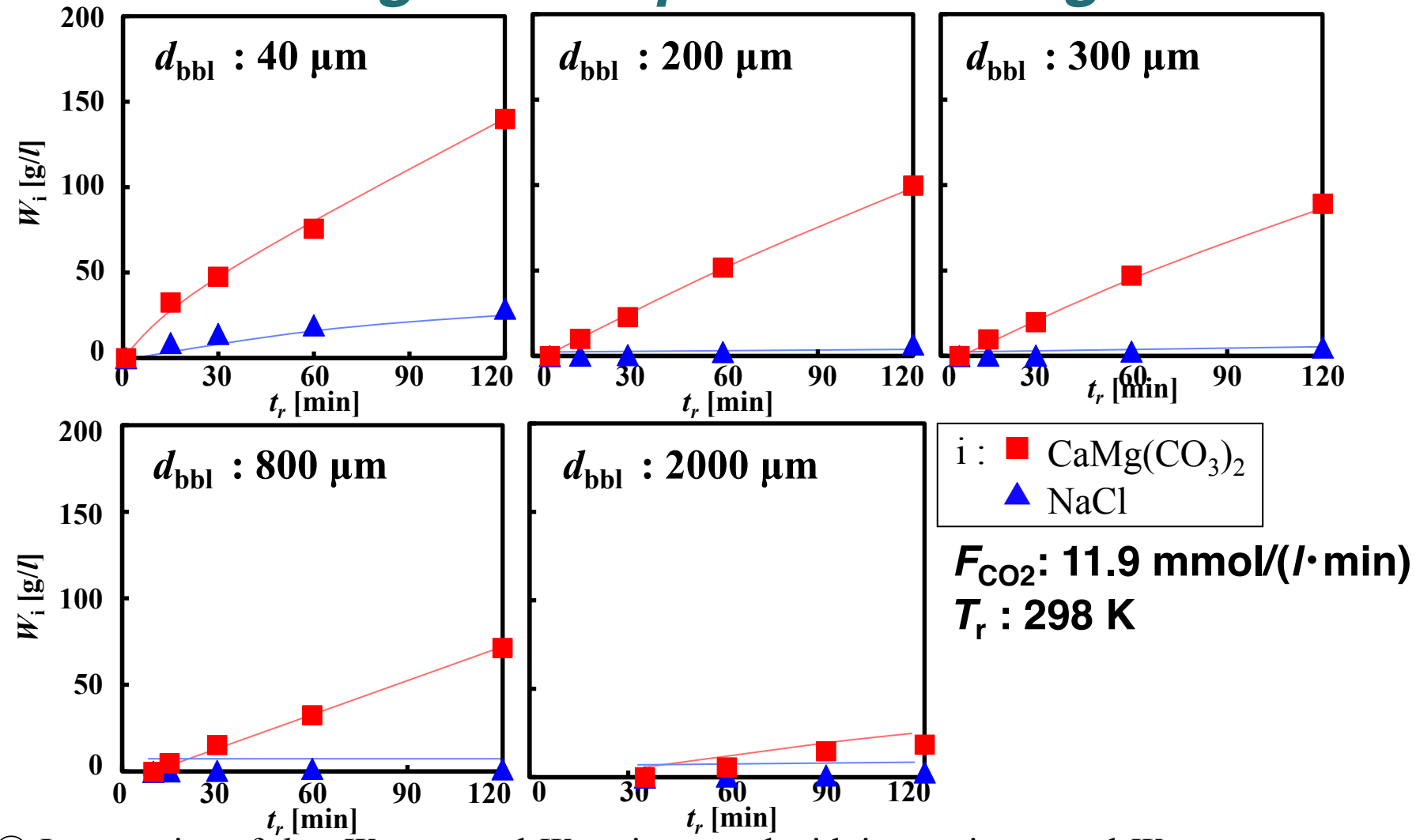

○ Irrespective of d_{bbl}, $W_{dolomite}$ and W_{NaCl} increased with increasing t_r, and $W_{dolomite}$ at d_{bbl} of 40 μm was obviously higher than the 2000 μm at all values of t_r.

○ The induction period for nucleation decreased with a decrease in d_{bbl}.

Effects of minimizing bubble diameter on time change in Mg/Ca ratio of $CaMg(CO_3)_2$

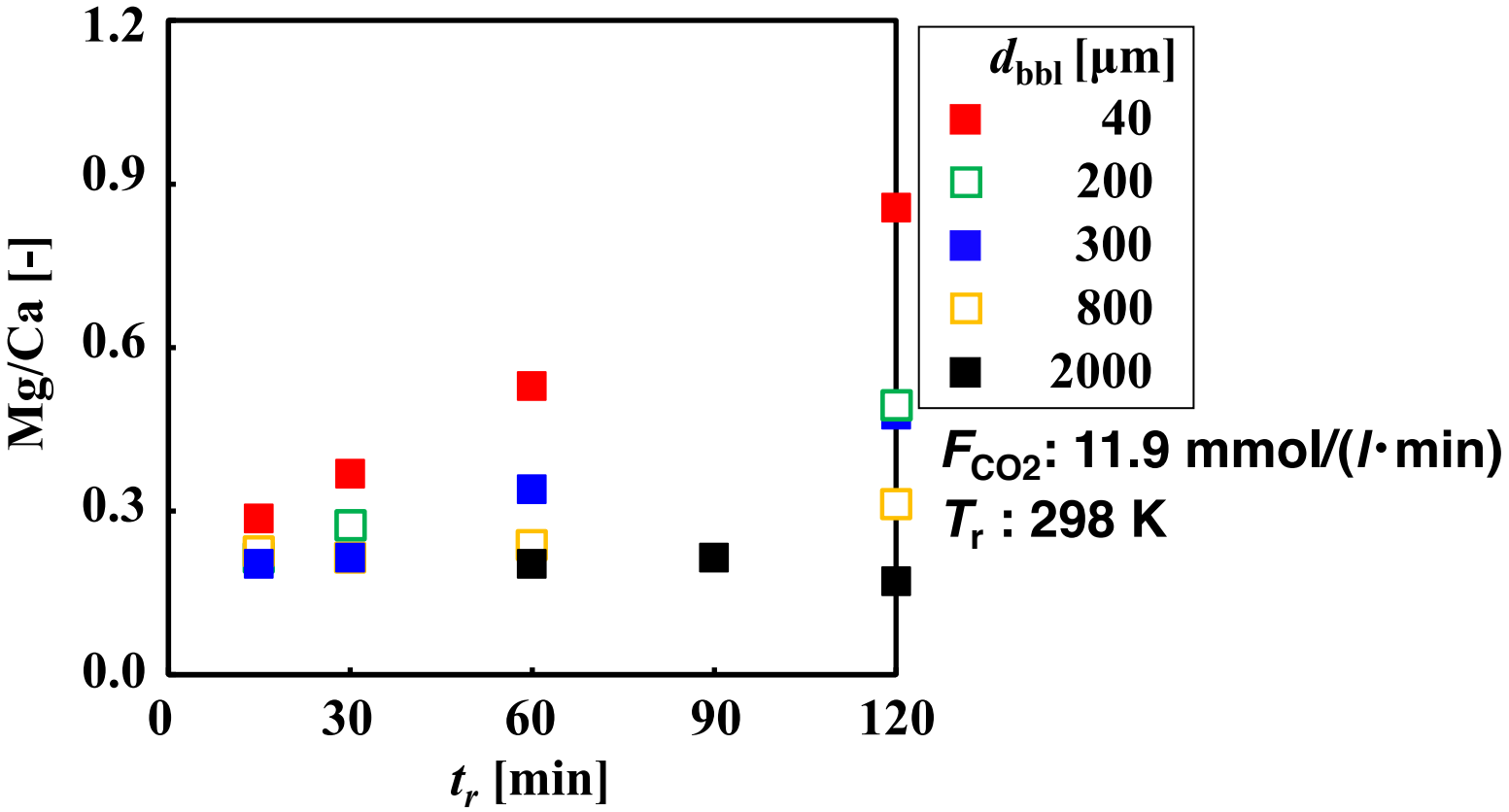

○ At d_{bbl} of 2000 μm Mg/Ca ratio of $CaMg(CO_3)_2$ remained almost constant at 0.20.

○ When d_{bbl} decreased to 40 μm, the Mg/Ca ratio increased linearly with t_r and was 0.86 at t_r of 120 min.

Comparison of SEM observation of $CaMg(CO_3)_2$ (t_r = 120 min)

F_{CO2}: 11.9 mmol/(*l*·min), T_r : 298 K

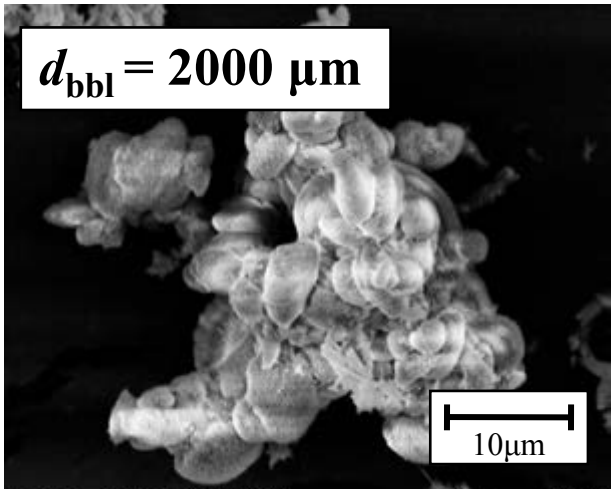

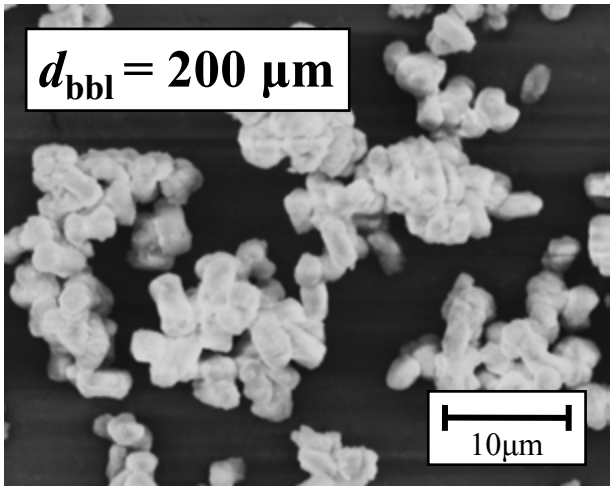

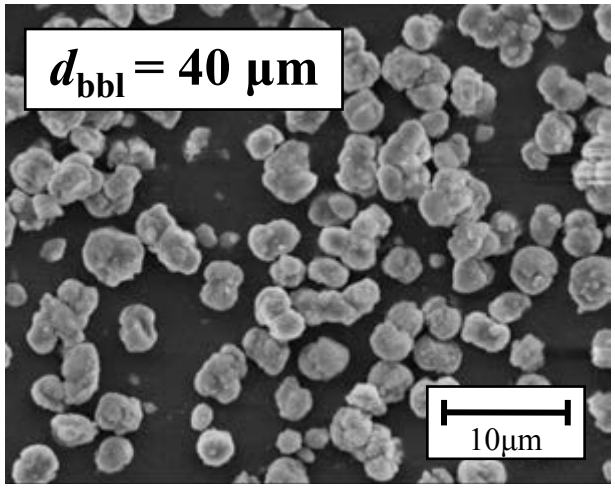

- At d_{bbl} of 2000 μm, the aggregate with an average size of approximately 20 μm was observed.
- When d_{bbl} was decreased to 40 μm, the spherical particles with a size of almost 2 μm were obtained.

Effects of CO_2 flow rate on produced weight, Mg/Ca ratio of $CaMg(CO_3)_2$ and induction time for nucleation (microbubble injection)

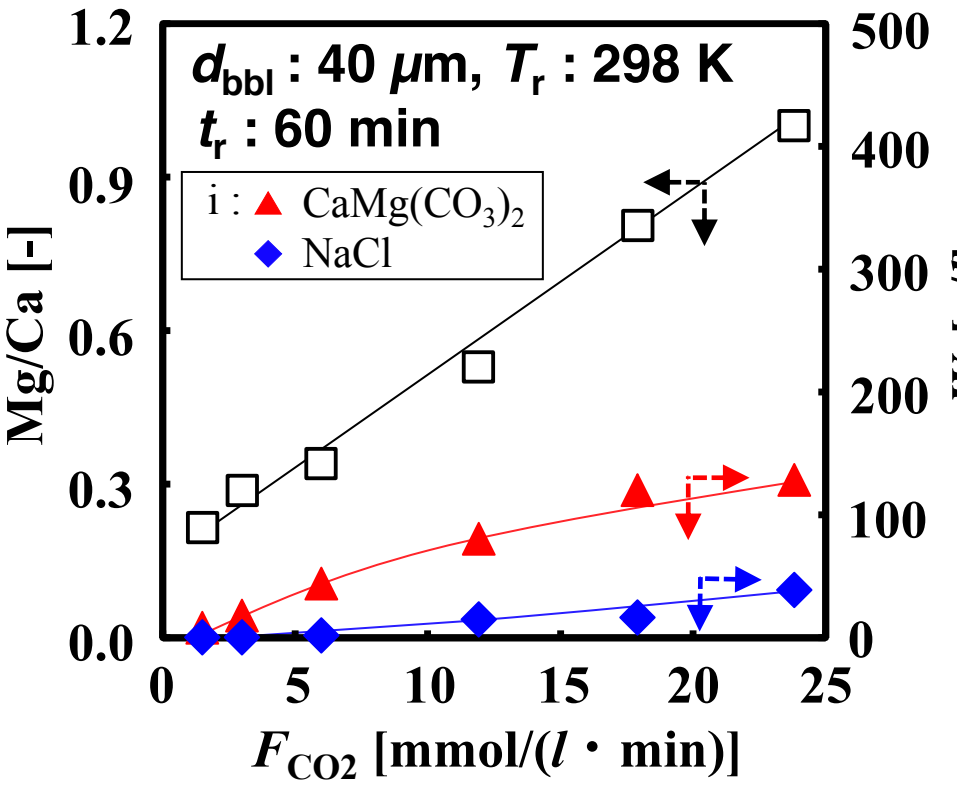

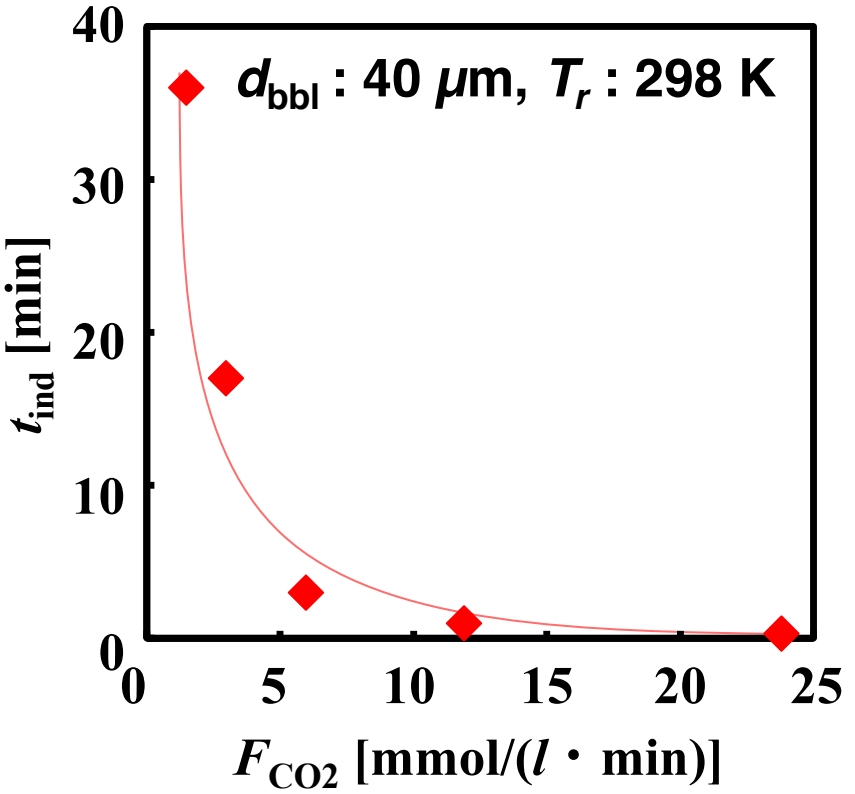

○ $W_{dolomite}$ and Mg/Ca ratio increased linearly with increasing F_{CO2}, and Mg/Ca ratio reached 1.0 in case where F_{CO2} was set at 23.8 mmol/(l·min).

○ The induction time for nucleation (t_{ind}) had a tendency to decrease when F_{CO2} was increased.

Effects of reaction temperature on produced weight, Mg/Ca ratio of $CaMg(CO_3)_2$ and induction time for nucleation (microbubble injection)

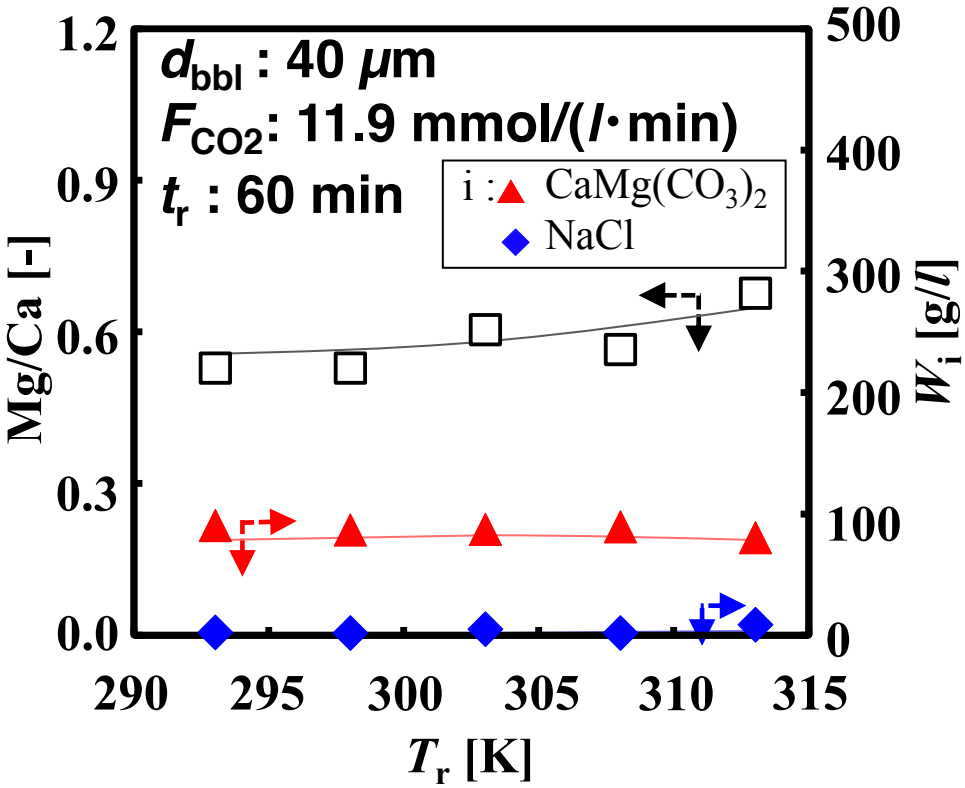

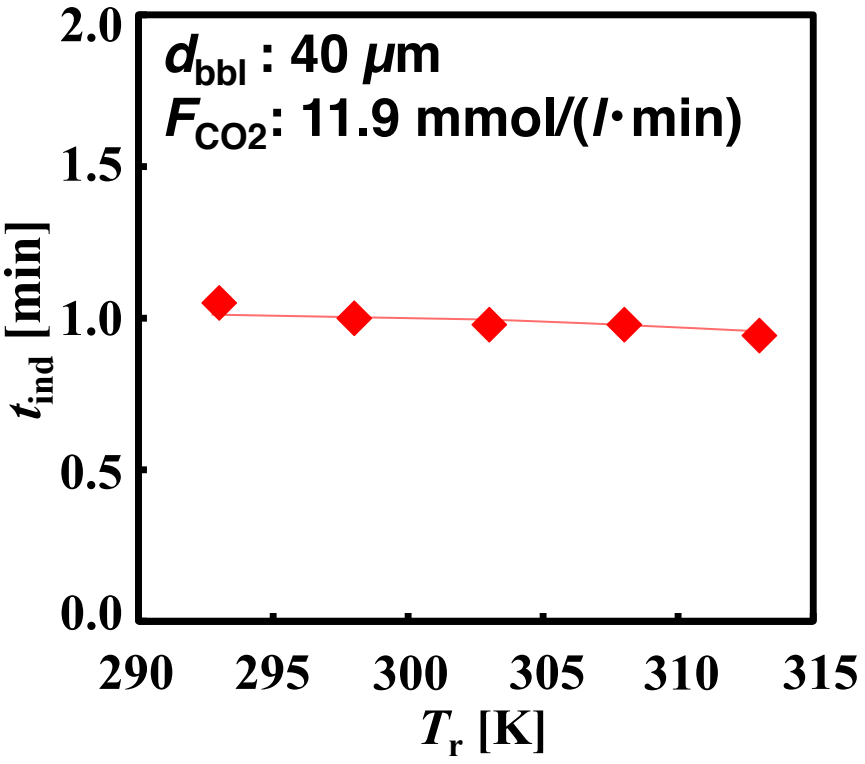

○ The change in $W_{dolomite}$ and t_{ind} was relatively small for all values of T_r.

○ Mg/Ca ratio of $CaMg(CO_3)_2$ increased gradually with an increase in T_r.

Relation between nucleation rate and increasing rate of Mg/Ca ratio

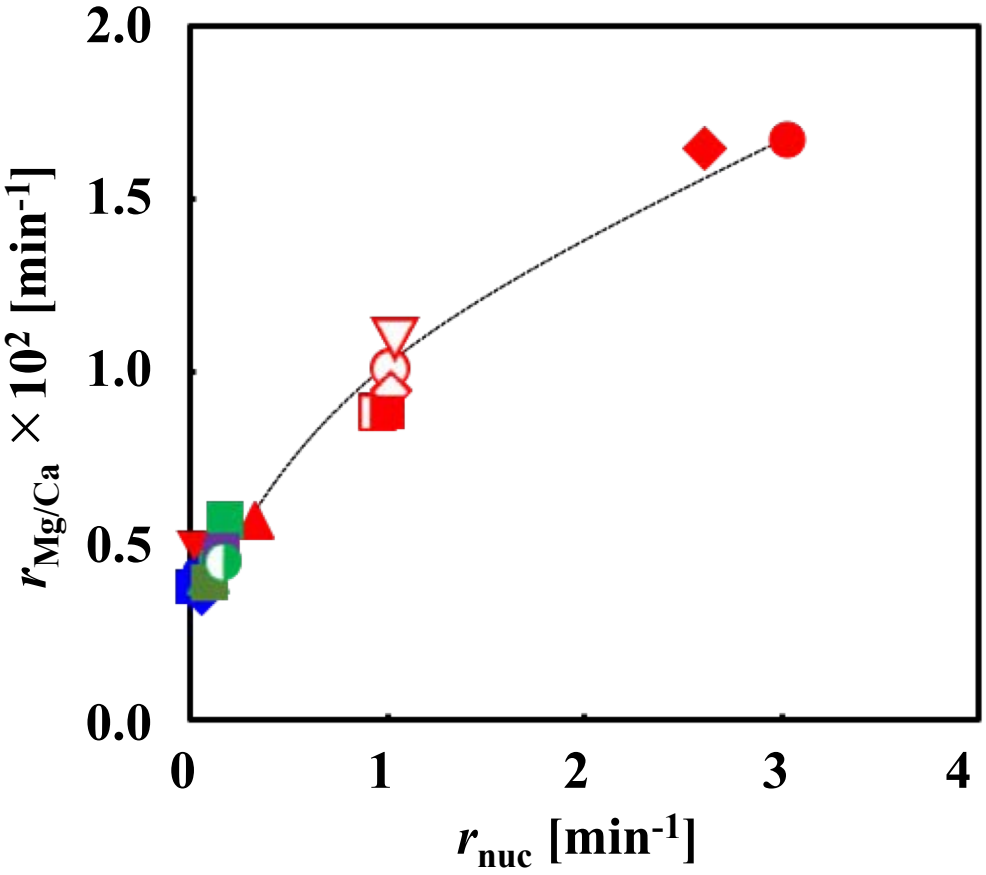

d_{bbl} [μm]	F_{CO2} [mM/min]	T_r [K] 293	298	303	308	313
40	1.49	-	▼	-	-	-
	2.58	-	◐	-	-	-
	5.96	-	▲	-	-	-
	11.9	□	■	▽	○	◇
	17.8	-	◆	-	-	-
	23.8	-	●	-	-	-

d_{bbl} [μm]	F_{CO2} [mM/min]	T_r [K] 298
200	11.9	■
300	5.96	▲
	8.93	◐
	11.9	■

d_{bbl} [μm]	F_{CO2} [mM/min]	T_r [K] 298
800	11.9	■
2000	8.93	◐
	11.9	■
	17.8	◆
	23.8	●

○ The increase in nucleation rate (r_{nuc}) caused by minimizing the bubble diameter is effective for realizing the higher Mg/Ca ratio.

Conclusion

- At a constant F_{CO2} of 11.9 mmol/ (l·min) and T_r of 298 K, the minimization of the bubble diameter led to the linear increase in $W_{dolomite}$ and Mg/Ca ratio and the micronization of $CaMg(CO_3)_2$.

  ➡ Because of the acceleration of CO_2 absorption and the electrification of the microbubble surface.

- When F_{CO2} was increased to 23.8 mmol/(l·min) at T_r of 298 K during reactive crystallization supplying CO_2 microbubbles with a d_{bbl} of 40 μm, the Mg/Ca ratio reached 1.0.

- During reactive crystallization with CO_2 microbubble injection, the dependence of Mg/Ca ratio on F_{CO2} was significantly greater than that of Mg/Ca ratio on T_r.

- Under the experimental conditions employed in the work, a positive correlation was observed between r_{nuc} and $r_{Mg/Ca}$.

⇨ **Microbubble injection that enables the acceleration of crystal nucleation is available for the high-yield crystallization of $CaMg(CO_3)_2$ fine particles with Mg/Ca ratio of 1.0.**

Acknowledgment

This work was financially supported by the Salt Science Research Foundation (Nos. 1523, 1620, 17A3, 18A3), Japan.

We also acknowledge the Naikai Salt Industry Co., Ltd. for provision of concentrated brine.

Characteristics of self-supporting bubble generator

O_2 gas flow rate [mmol/(l · min)] 0.56

DBD incident voltage [V] 60

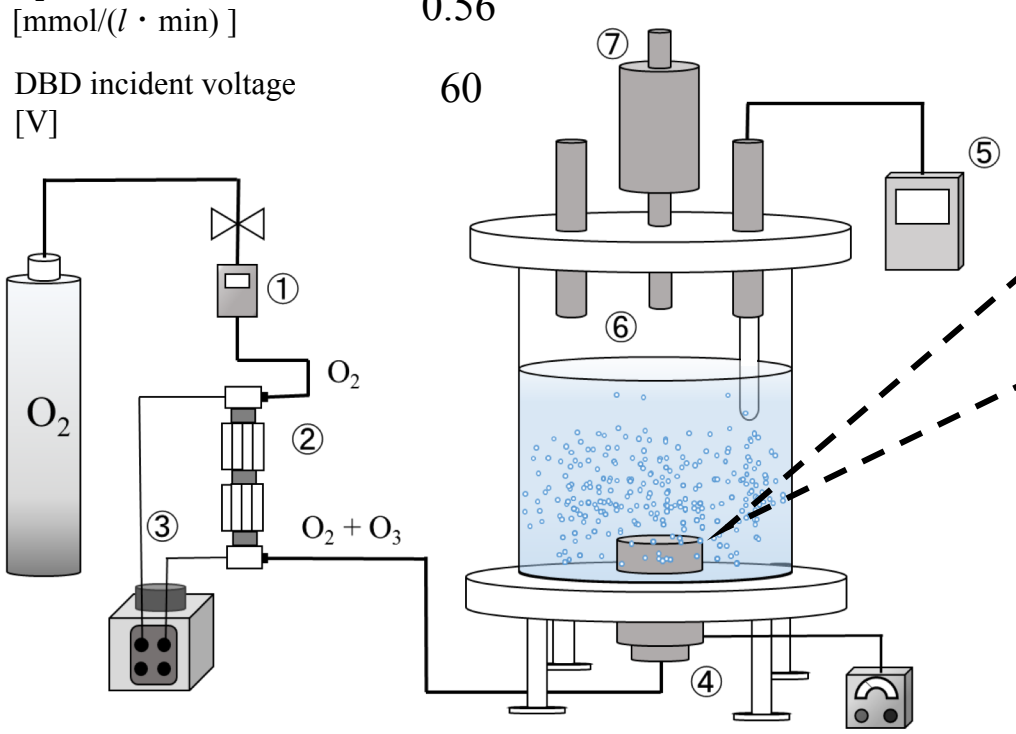

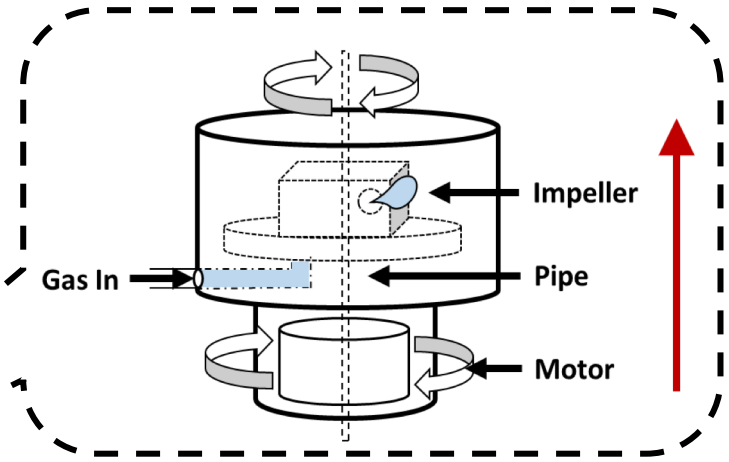

Without microbubbles

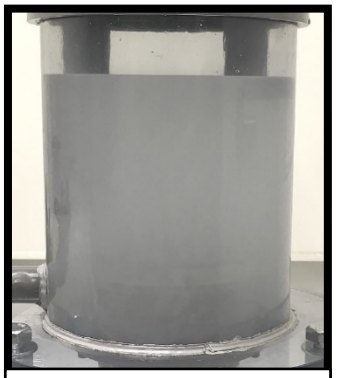

With microbubbles

① Mass-flow meter ② Dielectric Barrier Discharge (DBD) reactor
③ Transformer ④ Fine bubble generator ⑤ pH meter
⑥ Reaction vessel ⑦ Gas exit

○ Microbubbles with a d_{bbl} of 40 μm were generated using a self-supporting bubble generator by the shear of the impeller and a negative pressure owing to high-rotation.

Structure of microbubble generator

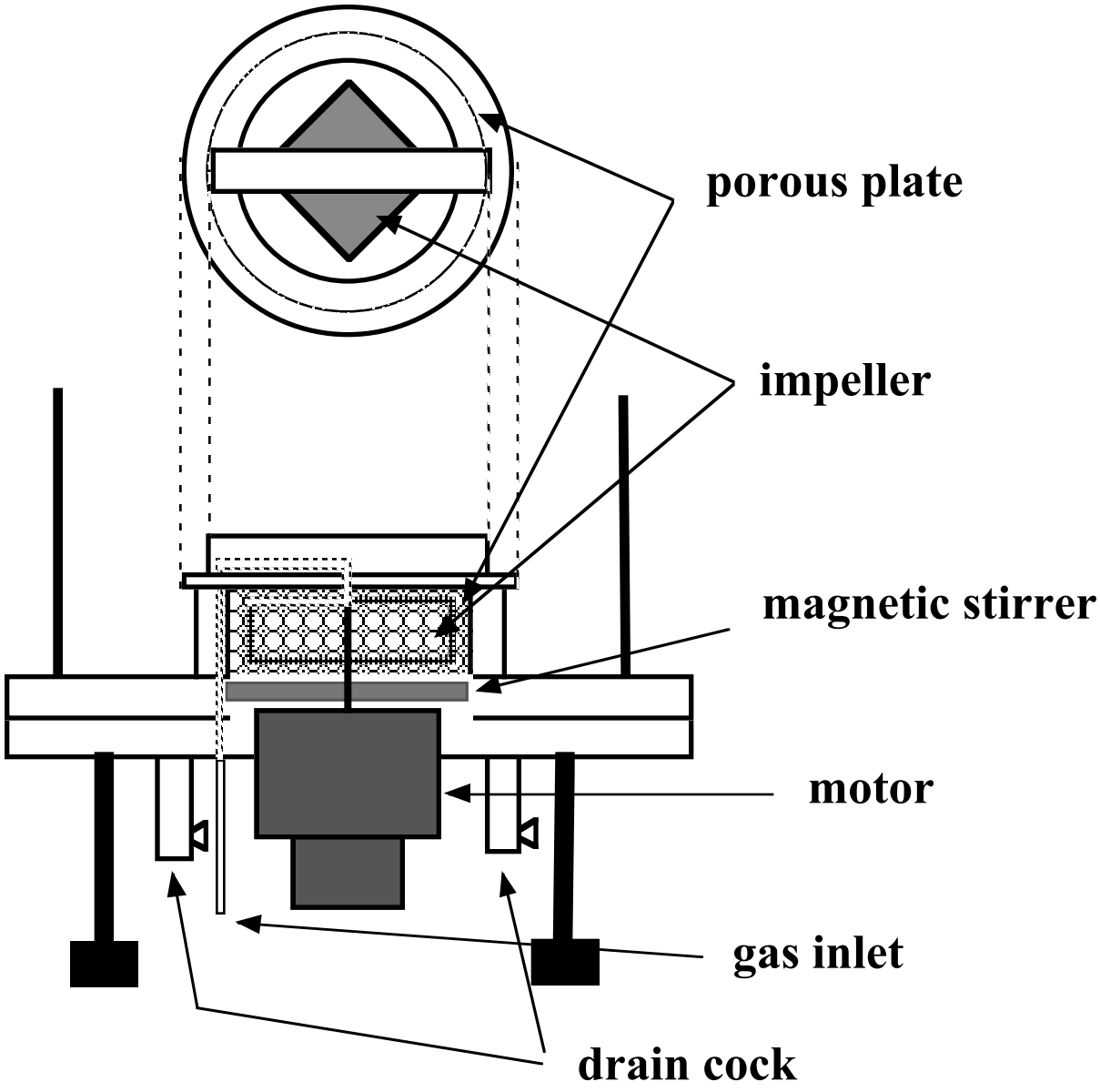

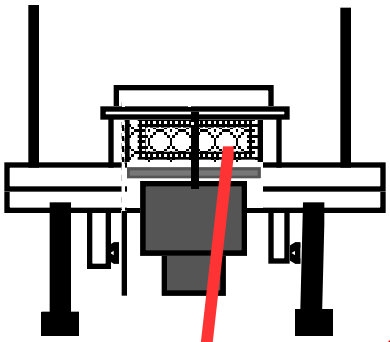

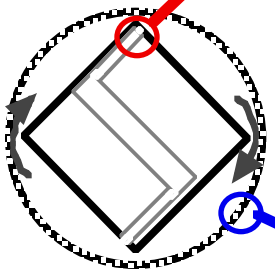

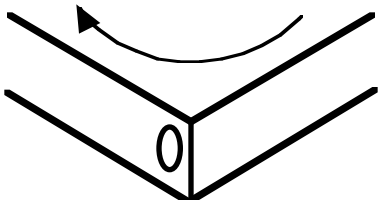

Bubble source gas is released from the impeller.

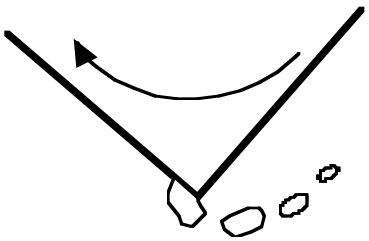

Gas is sheared by the rotation of the impeller.

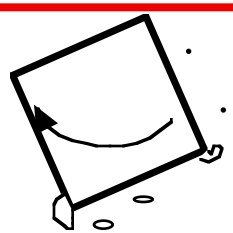

Gas is repetitively sheared, and bubble diameter is minimized.

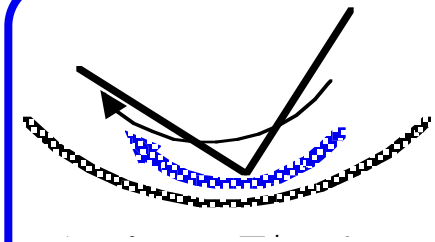

Heavy turbulence flow occurs near the porous plate caused by the rotation of impeller.

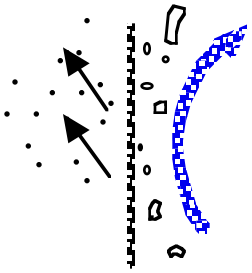

Only microbubbles pass through the porous plate.

★ Microbubbles with a d_{bbl} of 40 μm were generated using a self-supporting bubble generator by the shear of the impeller and a negative pressure owing to high-rotation.

Time change in pH and dissolved CO_2 (distilled water)

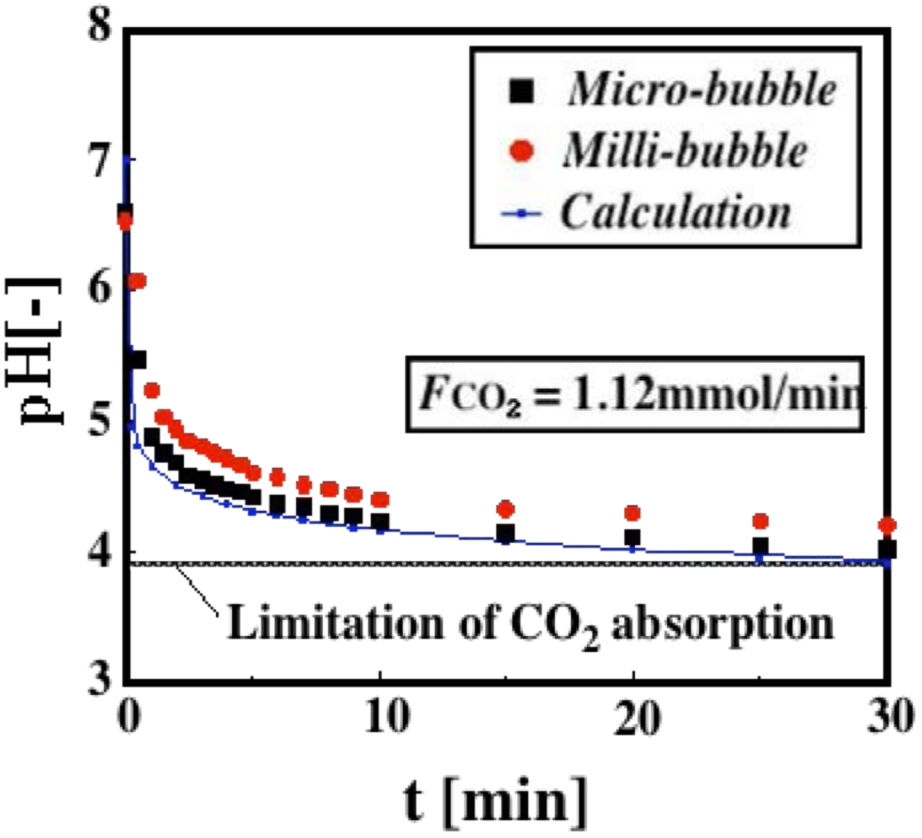

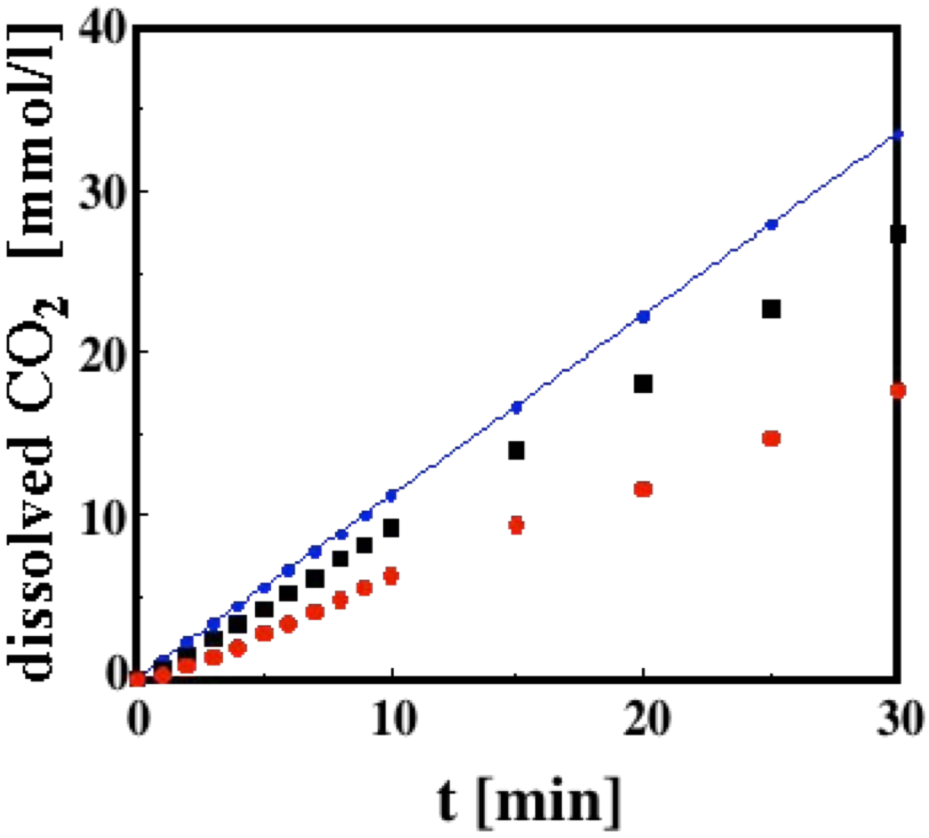

○ The concentration of dissolved CO_2 of micro-bubbles was higher than that of Milli-bubbles.

○ CO_2 dissolution ratio of micro and milli bubble were 85, 55% respectively.

Features of self-supporting micro-bubble generator

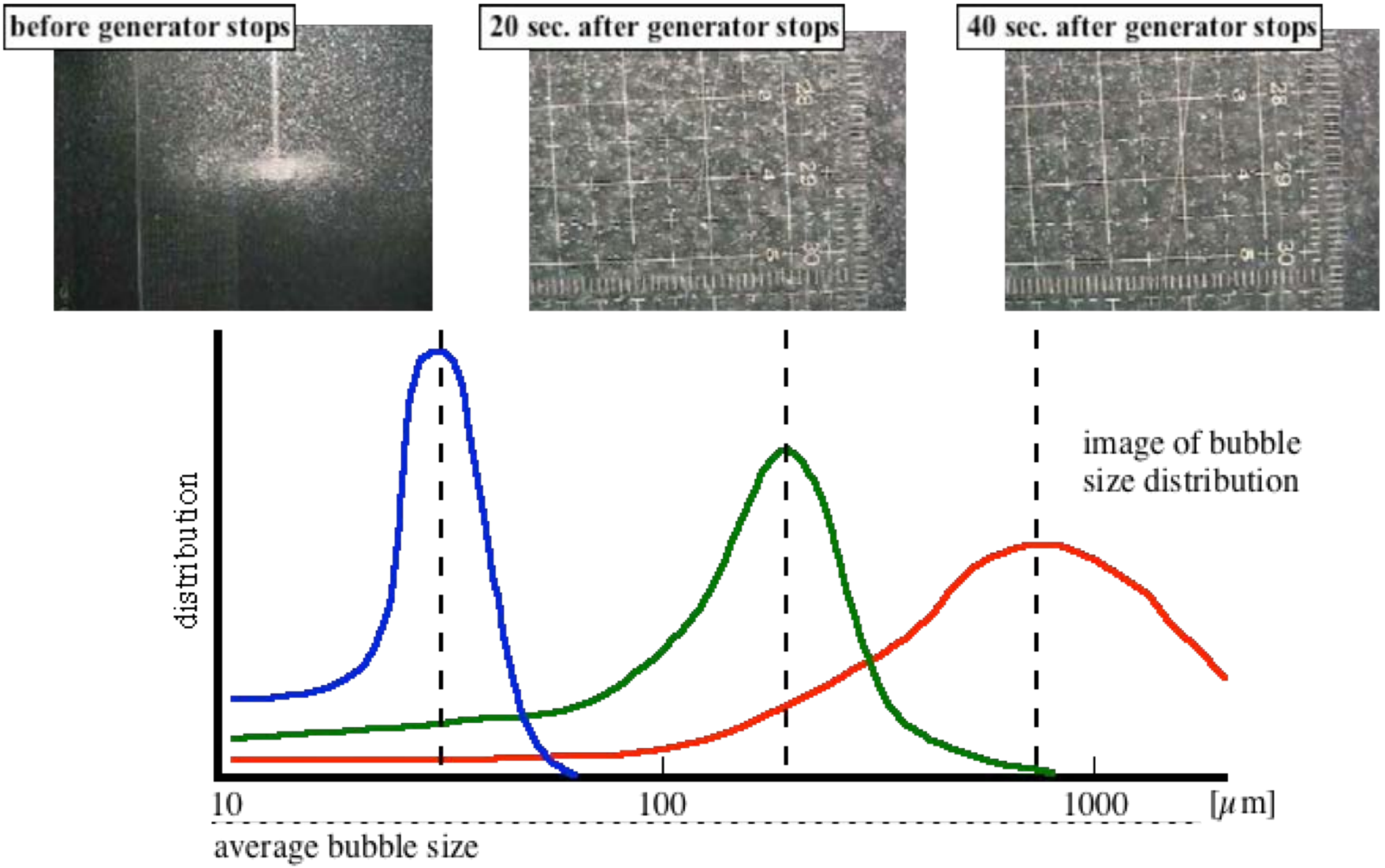

○ The average bubble size is variable in the range of 20 - 1000 μm by the controlling gas flow rate and rotation rate.

Comparison of bubble size distribution between self-supporting and distributor

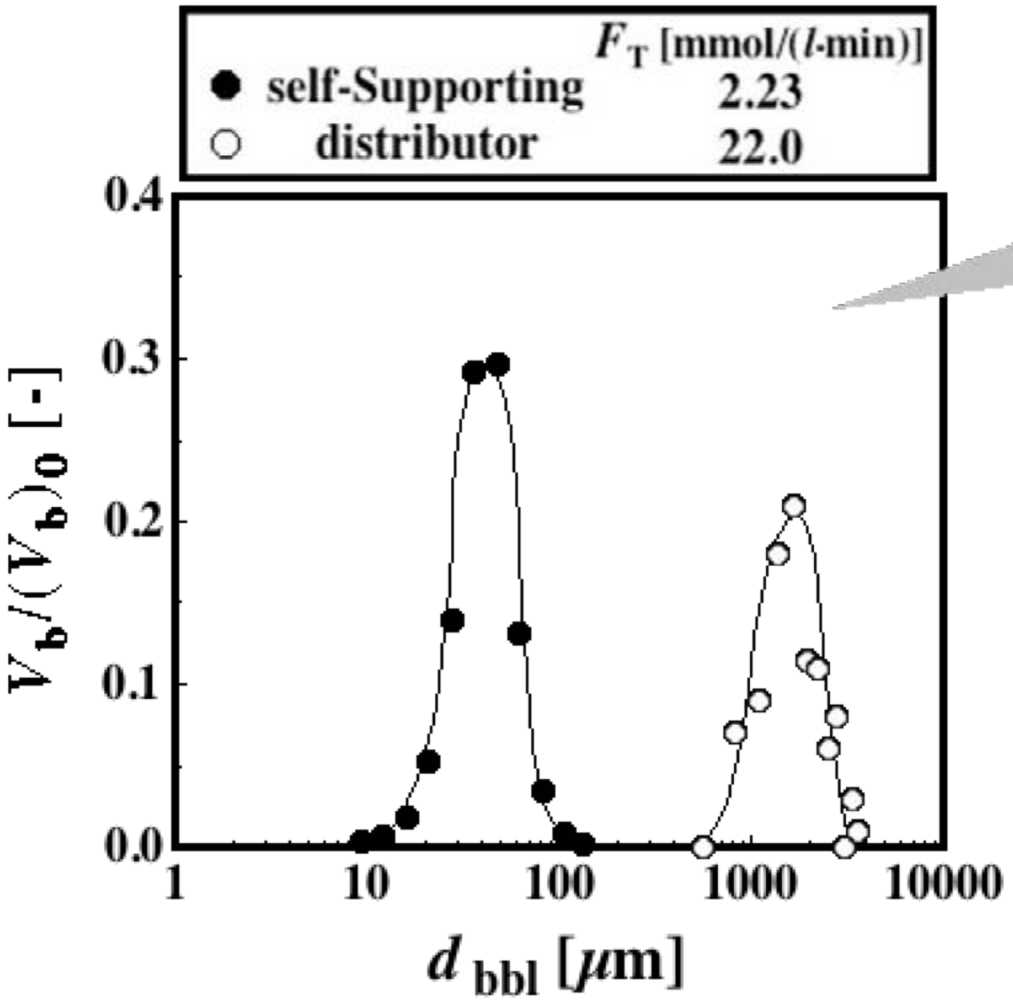

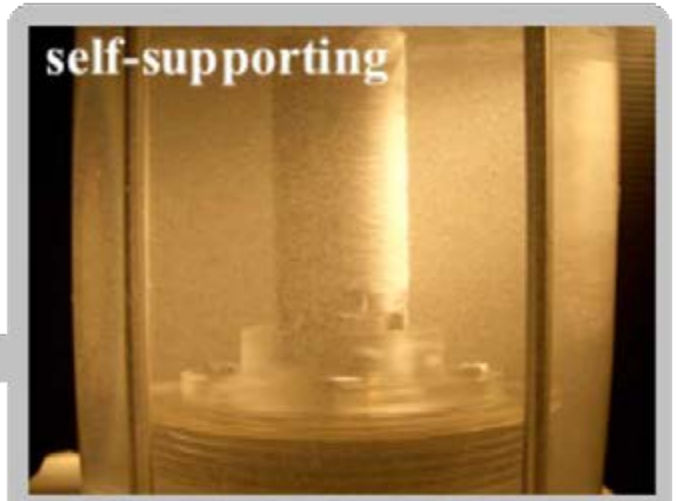

The mode size 40 μm

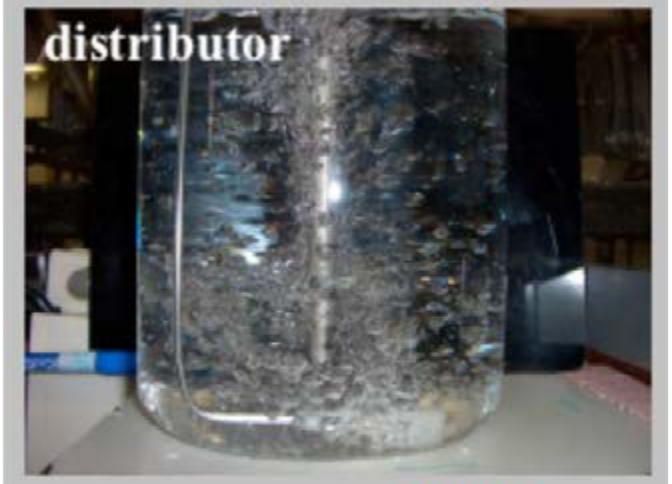

The mode size 2000 μm

Bubble size distribution of CO_2 micro bubbles (distilled water)

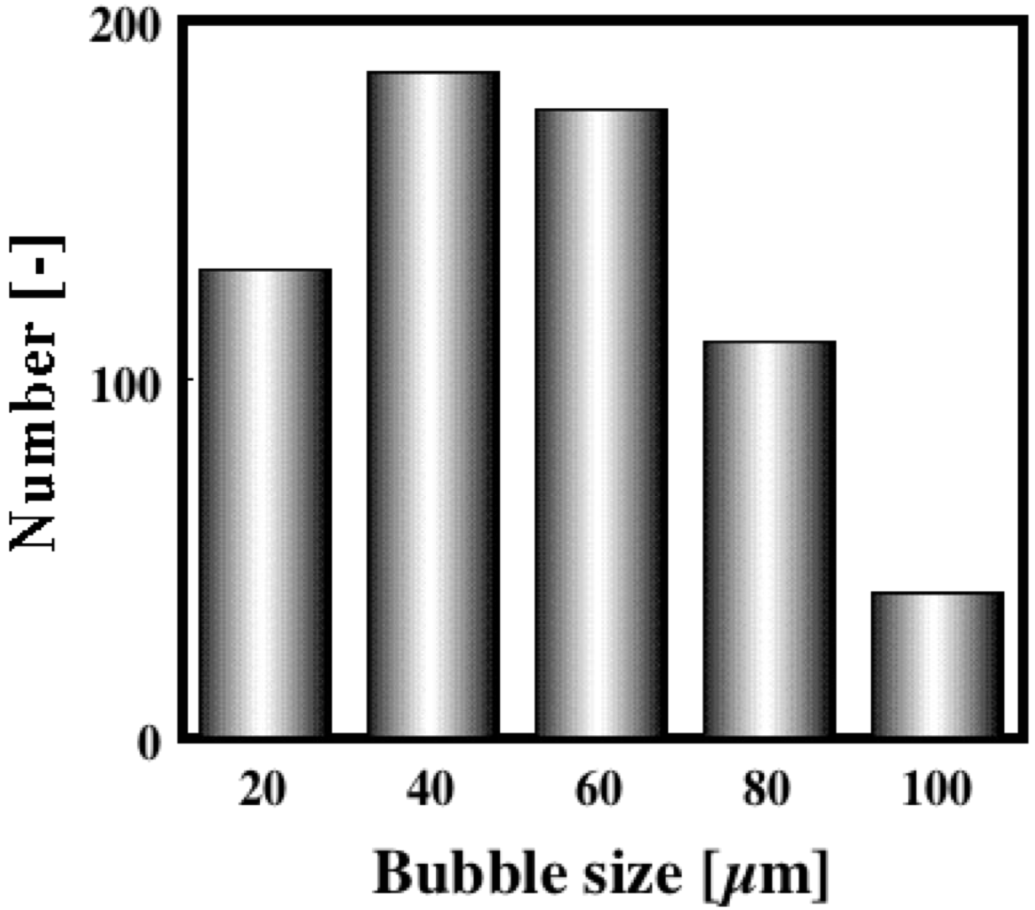

CO2 micro-bubble
***F*CO$_2$: 2.23mmol/min**

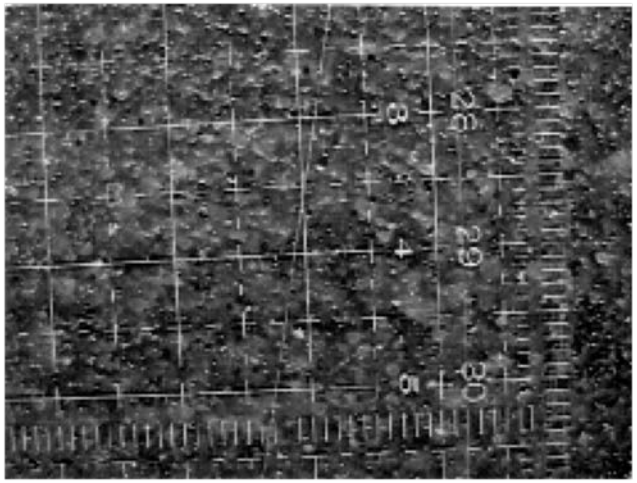

○ Bubble size distribution was measured by an image processing.

○ Bubble size was distributed below 100 μm, and the mode of bubble diameter showed 40 μm.

Comparison of bubble size distribution between self-supporting and distributor

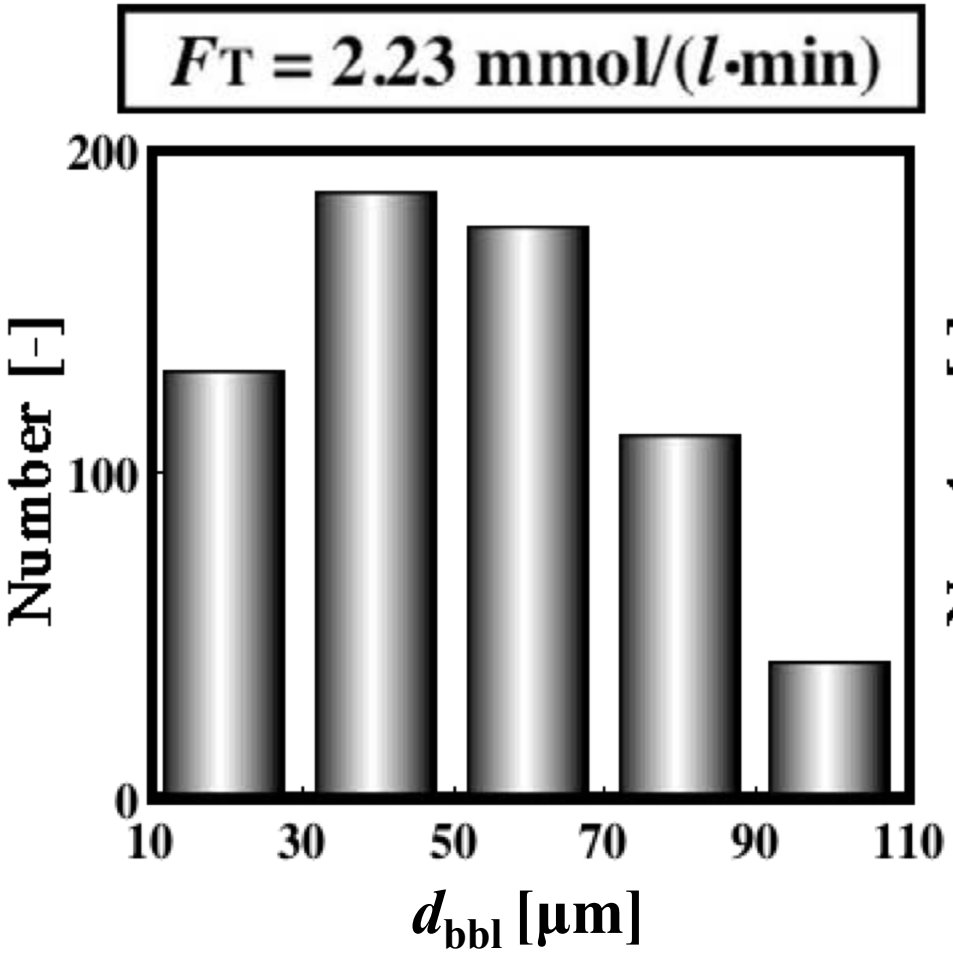

a) self-supporting

The mode of bubble diameter showd 40 μm

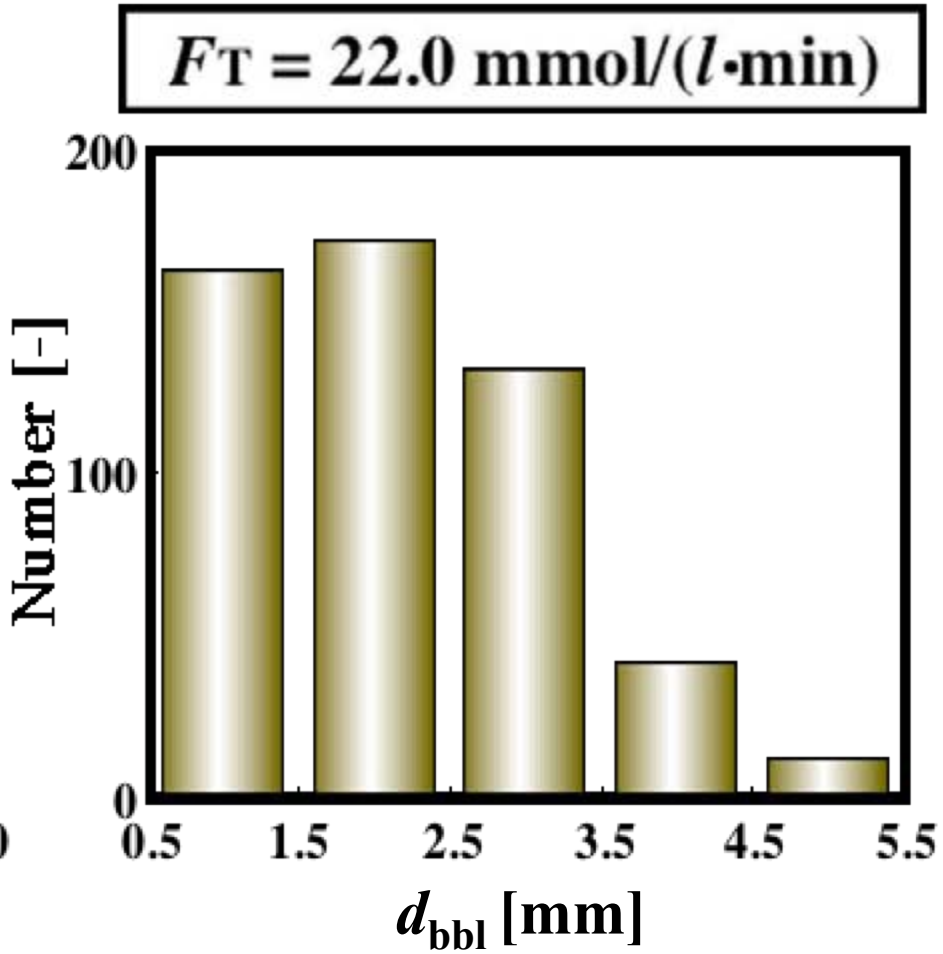

b) distributor

The mode of bubble diameter showd 2000 μm

Slow rising velocity

The rising velocity of an microbubble depends on the physical properties of liquids. For microbubbles of 100 μm diameter, Re number is nearly 1, and its shape is spherical. Such microbubbles behave as fluid spheres or solid spheres.
By the experimental results of the microbubbles rising velocity, both fluid and solid spherical behaviors were observed, while the rather many experimental results dollowing the Stokes equation applicatable to solid spheres are reported.

Table The rising velocity of microbubble in water(20℃) (following the Stokes equation)[1)]

Bubble diameter d_{bbl} [μm]	U [μm/s]	U [m/h]	Re number Re
100	5440	19.6	0.513
10	54.4	0.196	5.13×10^{-4}
1	0.544	1.96×10^{-3}	5.13×10^{-7}

★ The flotation rate at d_{bbl} of 10 μm is 100 times smaller than that of 100 μm.

1) "Micro- and Nanobubbles: Fundamentals and Applications", H. Tsuge (Ed.), Pan Stanford Publishing Pte. Ltd., Singapore (2014.8)

High pressure inside microbubbles (Self-compression effect)

Using Young-Laplace equation, the pressure in a bubble whose diameter is d_{bbl} increases to that lager than the surrounding pressure sue to the surface tension.

Table Relation between bubble inner pressure and bubble diameter [1)]

Bubble diameter d_{bbl} [μm]	Bubble inner pressure [atm]
1000	1.003
100	1.03
10	1.29
1	3.87
0.1	29.7

<Young-Laplace equation>

$$\Delta P_{bbl} = \frac{4\sigma}{d_{bbl}}$$

ΔP_{bbl} ：Pressure increase inside bubbles [Pa]
σ ：Surface tension [N/m]
d_{bbl} ：Bubble diameter [μm]

★ The inner pressure of microbubbles with a d_{bbl} of 10 μm increases to 1.29 atm in comparison with the surrounding pressure of microbubbles.

1) “Micro- and Nanobubbles: Fundamentals and Applications”, H. Tsuge (Ed.), Pan Stanford Publishing Pte. Ltd., Singapore (2014.8)

Large gas dissolution

Mass transfer rate from gas to liquid, or dissolving rate (N), is written by Eq.1 when the gas phase mass transfer resistance is neglected.

Table The liquid phase mass transfer coefficient k_L in O_2 micro-bubble – water system[1)]

Bubble diameter d_{bbl} [μm]	k_L [m/s]
1000	1.57×10^{-4}
100	1.81×10^{-4}
10	5.37×10^{-4}
1	5.20×10^{-3}

Equation 1

$$N = k_L A (p - p^*) / H$$

★ The mass transfer quantity of gas phase based on the unit time to the liquid phase increases 60,000-fold in the case where d_{bbl} is decreased from 1000 to 10 μm by assuming that the mass transfer resistance in the gas phase is negligible.

1) "Micro- and Nanobubbles: Fundamentals and Applications", H. Tsuge (Ed.), Pan Stanford Publishing Pte. Ltd., Singapore (2014)

Large gas dissolution

Table Comparison of mass transfer between milli-bubble and microbubble[1)]

Bubble diameter d_{bbl} [μm]	Rising velocity U [m/min]	ΔP [Pa]	Bubble number	Area ratio	Mass transfer ratio [mol/s]	Mass transfer ratio [mol/m]
1000	5.4	2.91×10^{2}	1	1	1	1
10	3.26×10^{-3}	2.91×10^{4}	1.0×10^{6}	100	6.15×10^{4}	1.0×10^{8}
0.1	3.26×10^{-3}	2.91×10^{6}	1.0×10^{12}	1.0×10^{4}	5.95×10^{10}	1.0×10^{18}

★ The mass transfer quantity of gas phase based on the unit time to the liquid phase increases 60,000 times in the case where d_{bbl} is decreased from 1000 to 10 μm by assuming that the mass transfer resistance in the gas phase is negligible.

★ The flotation rate of bubbles at a d_{bbl} of 10 μm in the water decreases to 1/1700 and the mass transfer quantity based on a unit flotation distance increases to 10 million times compared with the mass transfer quantity of 1000 μm.

1) "Micro- and Nanobubbles: Fundamentals and Applications", H. Tsuge (Ed.), Pan Stanford Publishing Pte. Ltd., Singapore (2014.8)

Effects of solution pH on reactive crystallization of $CaMg(CO_3)_2$ with CO_2 microbubble injection

Experimental apparatus and conditions

Major components of concentrated brine

Element	Conc. [mol/*l*]
Ca^{2+}	0.67
Mg^{2+}	2.1
Na^{+}	0.84
Cl^{-}	7.1

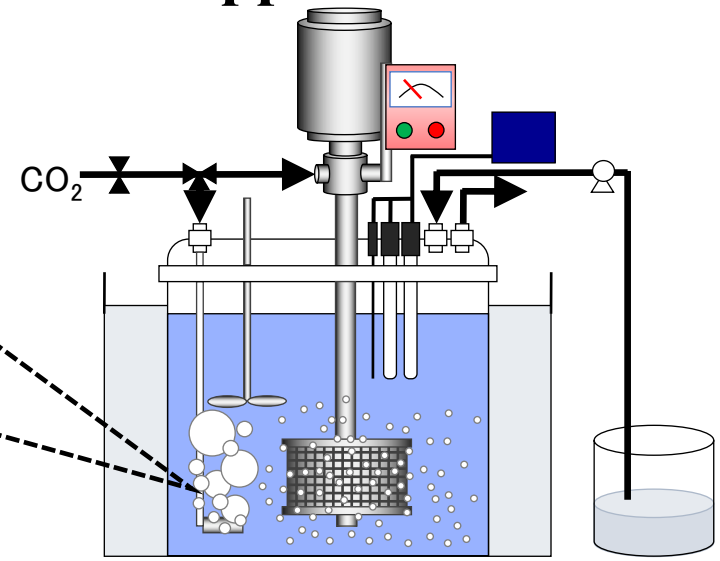

Method	Microbubbles
Bubble generator	Self-supporting
Average bubble size (d_{bbl}) [μm]	**40**
Rotation rate [min^{-1}]	1500
pH adjustment	
NaOH aqueous solution [mol/*l*]	4.0
CO_2 flow rate (F_{CO2}) [mmol/(*l*·min)]	11.9
Reaction pH [-]	**4.3-8.3**
Reaction temperature (T_r) [K]	**298**
Reaction time (t_r) [min]	0 - 60

Effects of solution pH on time changes in molar concentration of solid produced

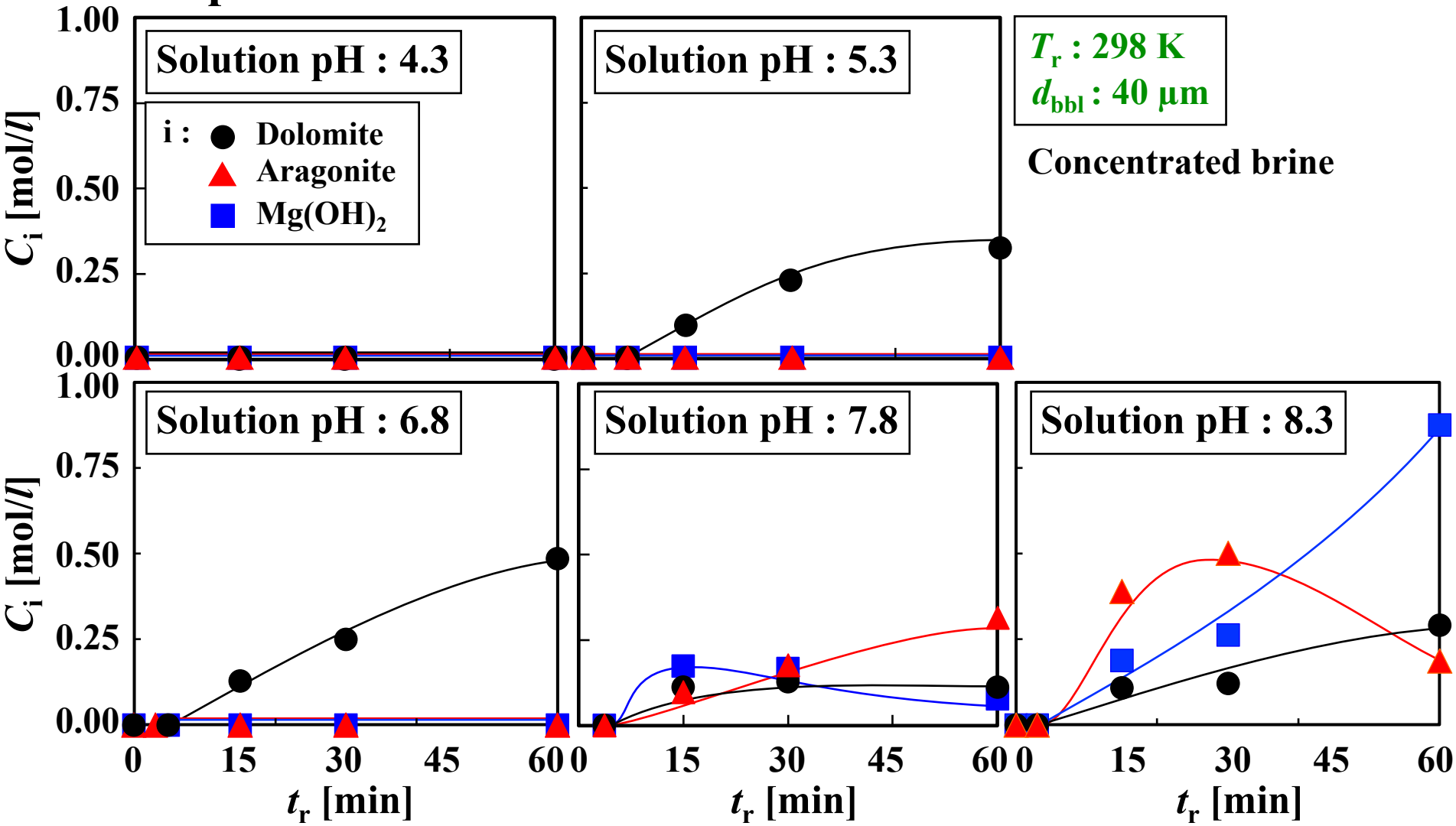

◯ At pH of 4.3, the solid product was not obtained within the crystallization time of 60 min.

◯ At pH of 5.3, $C_{dolomite}$ was increased with the progress of crystallization.

◯ At pH of 8.3, $CaMg(CO_3)_2$, aragonite and $Mg(OH)_2$ were produced.

Relation between solution pH and molar concentration of solid produced

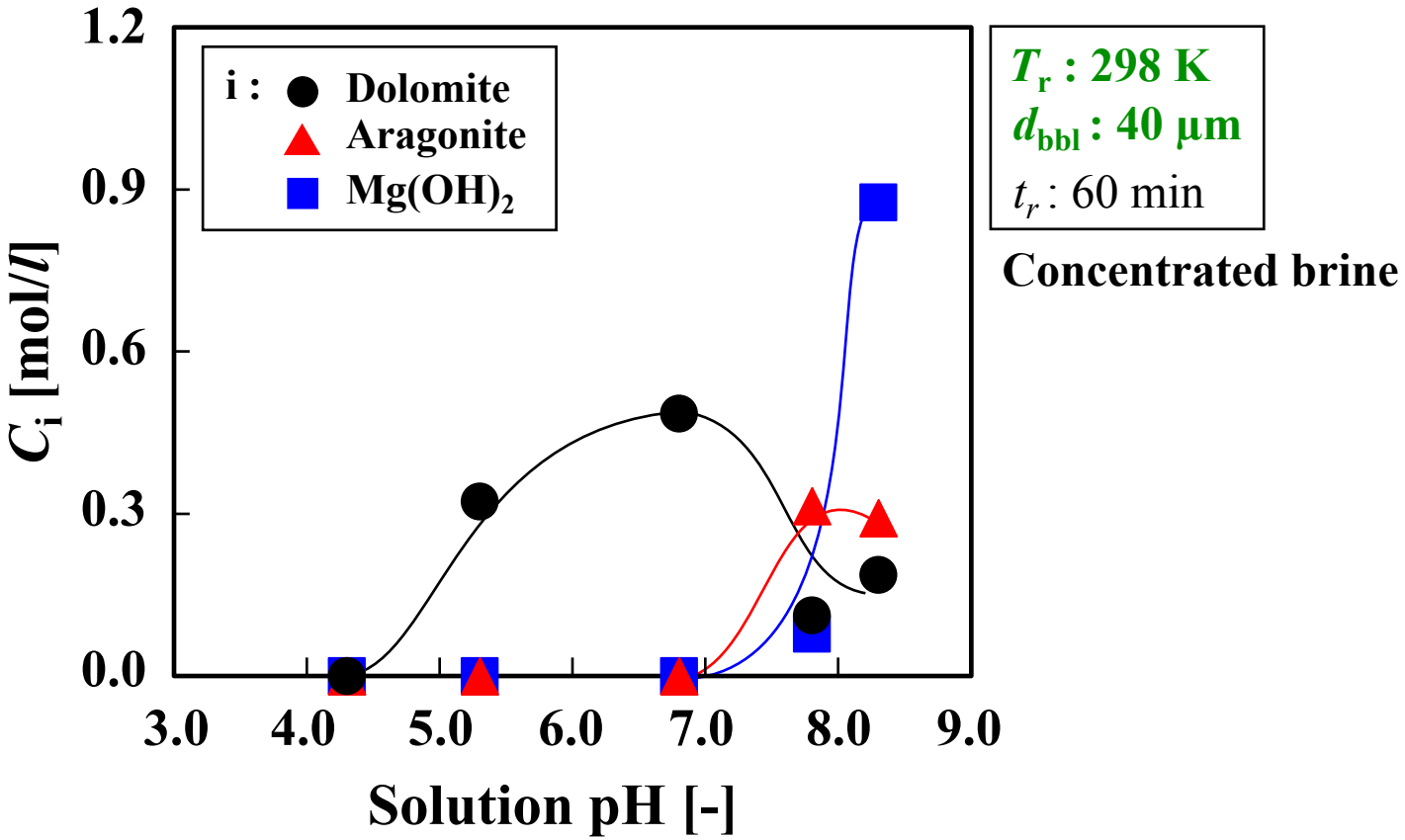

- $C_{dolomite}$ and $C_{aragonite}$ showed the maximum values at solution pH of 6.8 and 7.8, respectively.
- In the pH range over 7.3, $C_{Mg(OH)2}$ was increased with an increase of pH.

Effects of reaction temperature on reactive crystallization of $CaMg(CO_3)_2$ with CO_2 microbubble injection

Experimental apparatus and conditions

Major components of concentrated brine

Element	Conc. [mol/*l*]
Ca^{2+}	0.67
Mg^{2+}	2.1
Na^{+}	0.84
Cl^{-}	7.1

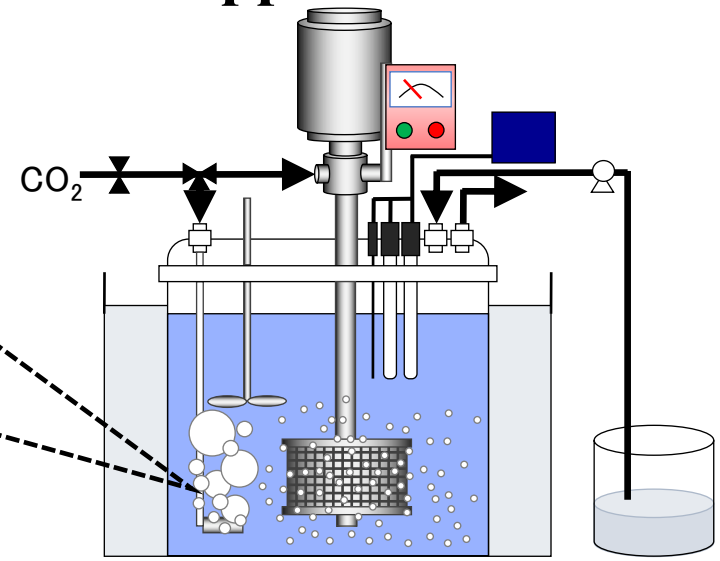

Method	Microbubbles
Bubble generator	Self-supporting
Average bubble size (d_{bbl}) [μm]	**40**
Rotation rate [min^{-1}]	1500
pH adjustment	
NaOH aqueous solution [mol/*l*]	4.0
CO_2 flow rate (F_{CO2}) [mmol/(*l*・min)]	11.9
Reaction pH [-]	**5.3**
Reaction temperature (T_r) [K]	**278-348**
Reaction time (t_r) [min]	0 - 60

Effects of reaction temperature on time changes in molar concentration of solid produced

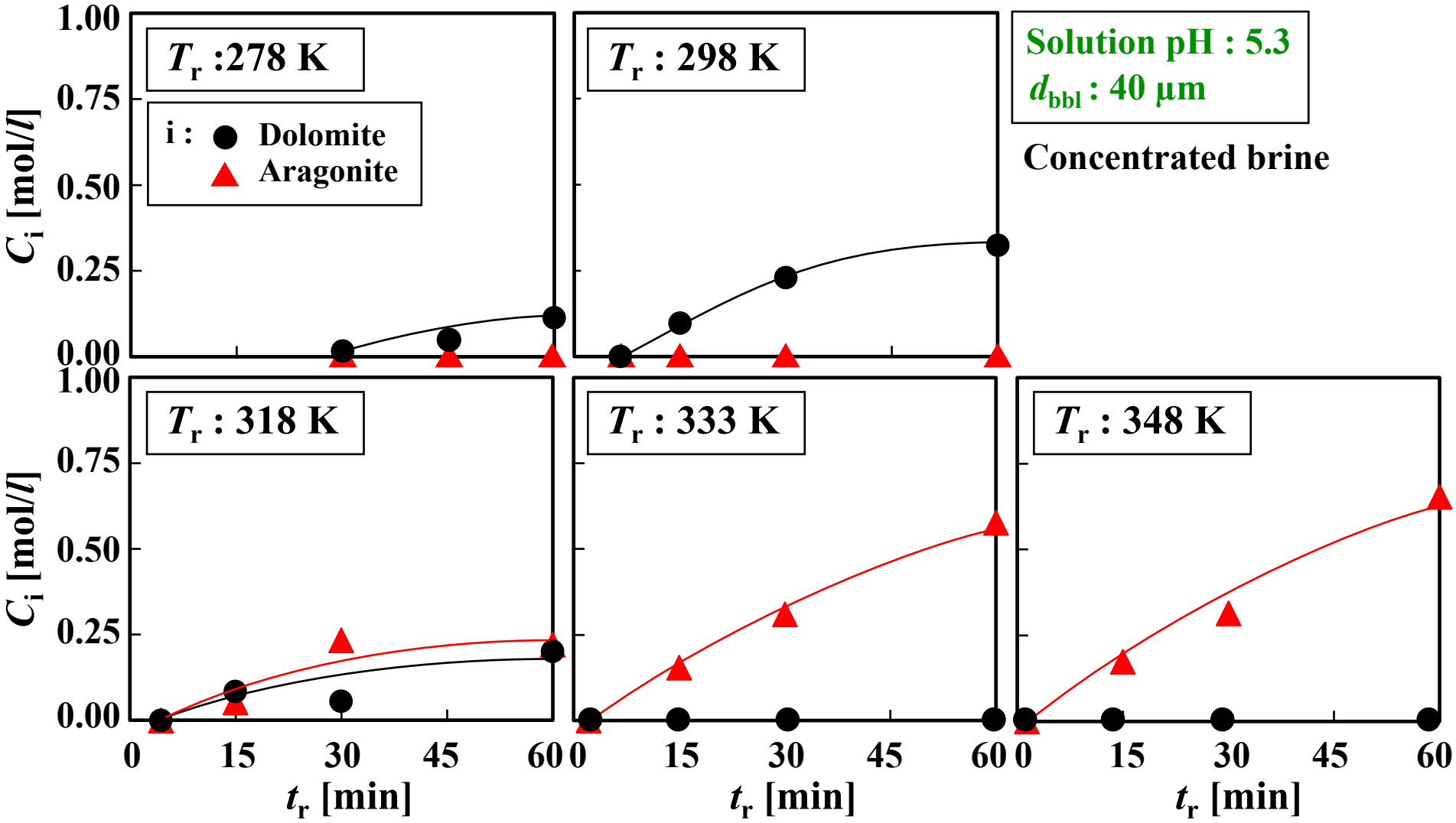

◯ At T_r of 278 K, $G_{dolomite}$ was slightly increased with the progress of crystallization.

◯ When T_r was rised to 298 K, the increasing tendency of $G_{dolomite}$ for t_r became significant.

◯ At T_r of 333 K, aragonite was selectively crystallized.

Relation between reaction temperature and molar concentration of solid produced

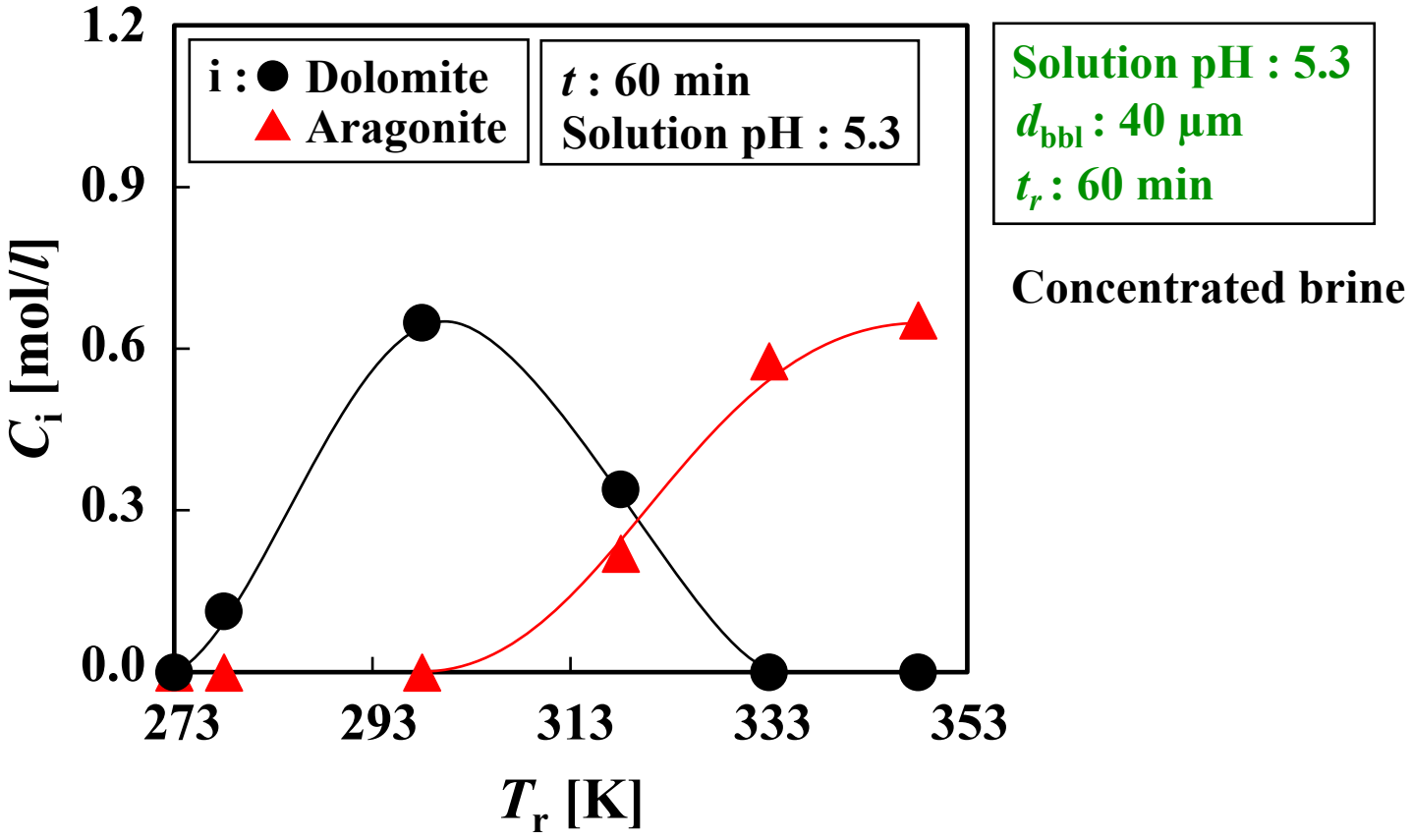

◯ $C_{dolomite}$ showed a maximum value at T_r of 298 K.

◯ In the T_r range over 313 K, $C_{aragonite}$ was increased with an increase of T_r.

Relations between solution pH, reaction temperature and molar concentration of solid produced

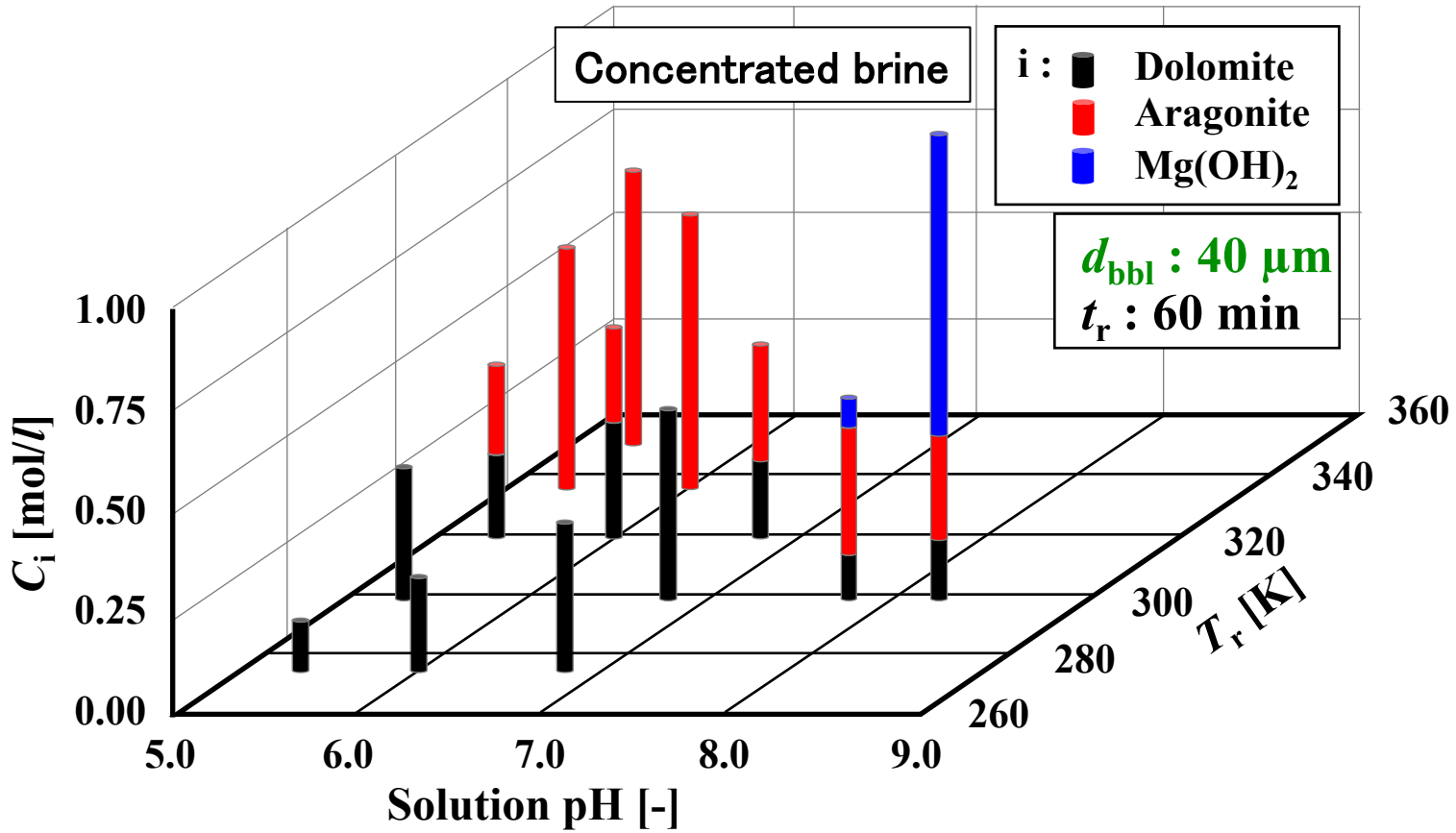

- ◯ At pH of 5.3–6.8 and T_r of 278–298 K, $CaMg(CO_3)_2$ was mainly product.
- ◯ At pH of 5.3, the production of aragonite was accelerated by increasing the T_r.
- ◯ At T_r of 298 K and pH of 7.8, $CaMg(CO_3)_2$, aragonite and $Mg(OH)_2$ were produced.

Synthesis of $CaMg(CO_3)_2$ from $CaCO_3$ seed crystals

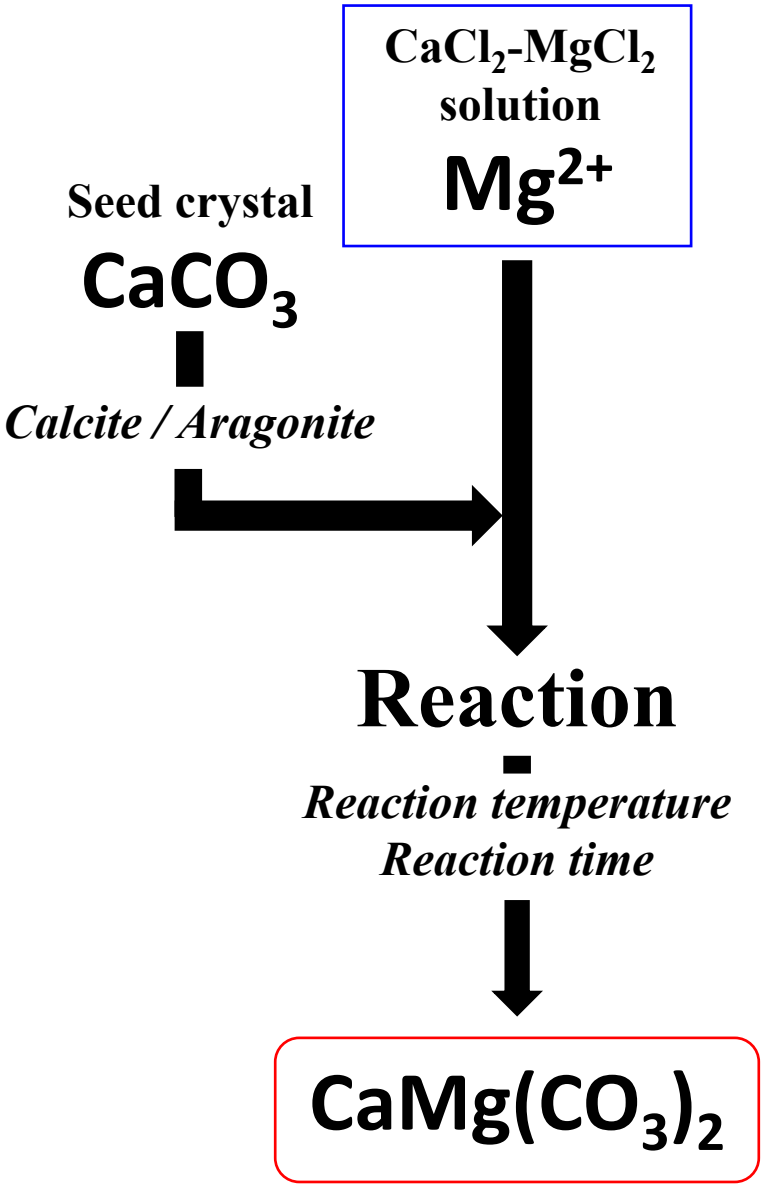

Experimental conditions

Solid reactant ($CaCO_3$) [mg]	50
Volume [ml]	5
Temperature [K]	525 - 568
Reaction time [h]	0.1 - 188.5
Solution concentration [mol/*l*]	
$CaCl_2$	1.6
$MgCl_2$	0.4
Mg/Ca ratio in solution [-]	0.26

◯ $CaCO_3$ crystals were suspended in $CaCl_2$–$MgCl_2$ solution and were transformed to $CaMg(CO_3)_2$.

6) A. Katz *et al., Geochimical et Cosmochimica. Acta*, **41**, pp. 297 - 308, (1977)

Effects of reaction time on solid products

Seed crystal : Calcite

Time [h]	Solid products	Mg/Ca
6.00	C	0.067
32.00	C, HMC	0.10
48.00	C, HMC	0.15
64.00	C, HMC	0.29
72.00	C, HMC, D	0.35
88.00	C, HMC, D	0.76
96.00	C, HMC, D	0.95
112.00	D	1.0
170.00	D	1.0

(C : Calcite HMC : High magnesium calcite D : Dolomite)

Relation between reaction time and mole fraction of solid products*

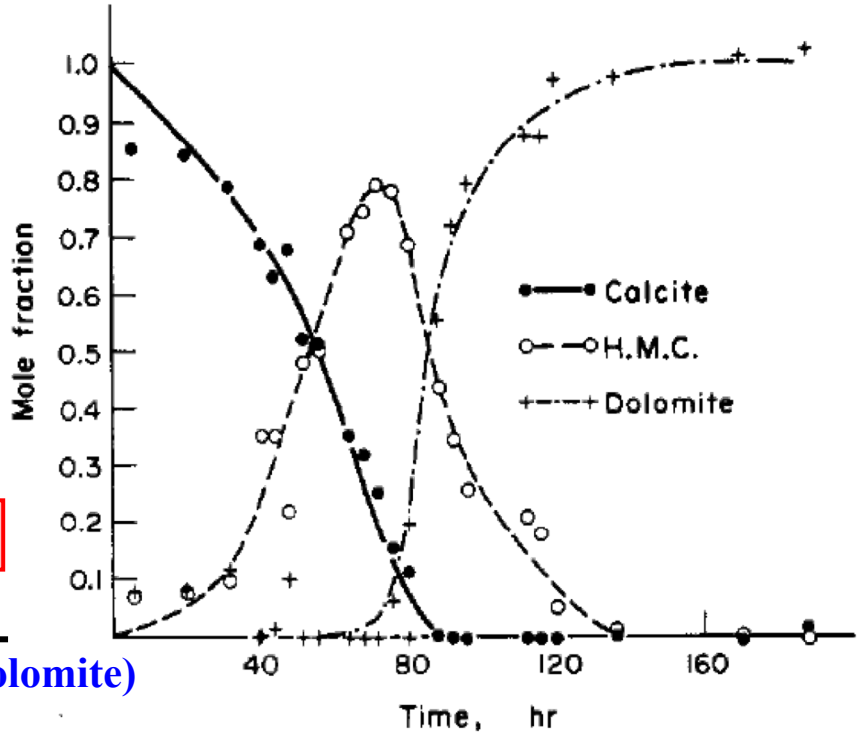

- The experimental synthesis of $CaMg(CO_3)_2$ via replacement of the calcite reactant is extremely slow and proceeds through the intermediate disordered phases are changed in the order of the calcite, high magnesium calcite.
- $CaMg(CO_3)_2$ was obtained from the calcite because the replacement of Ca^{2+} to Mg^{2+} progresses via the Ca^{2+} elution and Mg^{2+} inclusion.
- The reaction time of 96 h is necessary for the synthesis of $CaMg(CO_3)_2$ with a Mg/Ca ratio of 0.9–1.0 at a reaction temperature of 296 K.

* A. Katz *et al., Geochimical et Cosmochimica. Acta*, **41**, pp. 297 - 308, (1977)

Effects of $CaCO_3$ polymorphs on $CaMg(CO_3)_2$ production

Seed crystal : **Calcite**

Time [h]	Solid products	Mg/Ca
6.00	C	0.067
20.25	C	0.073
32.00	C, HMC	0.10
40.50	C, HMC	0.12
48.00	C, HMC	0.15
56.00	C, HMC	0.21
64.00	C, HMC	0.29
72.00	C, HMC, D	0.35
80.00	C, HMC, D	0.52
88.00	C, HMC, D	0.76
96.00	C, HMC, D	0.95
112.00	D	1.0
120.00	D	1.0
170.00	D	1.0

Seed crystal : **Aragonite**

Time [h]	Solid products	Mg/Ca
0.10	A, LMC	0.058
1.00	LMC	0.12
2.00	LMC, HMC	0.17
4.00	LMC, HMC	0.26
8.00	LMC, HMC, D	0.35
12.00	LMC, HMC, D	0.52
16.25	LMC, HMC, D	0.73
20.20	LMC, HMC, D	
24.25	D	1.0
30.00	D	1.0
69.00	D	0.91

(LMC : Low magnesium calcite)

⇨ $CaMg(CO_3)_2$ recrystallized after the dissolution of seed crystals into $CaCl_2$–$MgCl_2$ solution.

Comparison of time changes in the added moles of NaOH

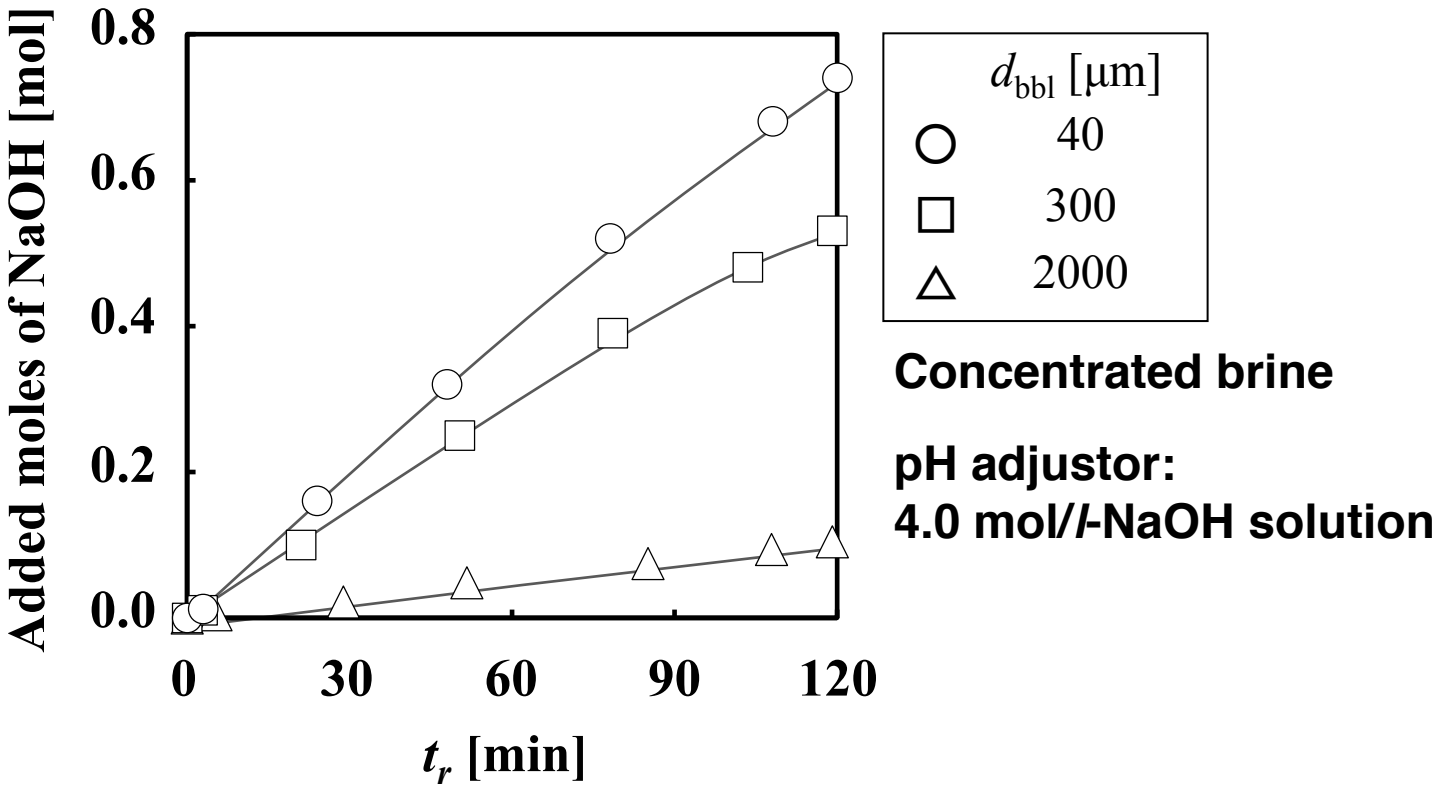

○ The added moles of NaOH as pH adjustor were increased because of the augment in CO_2 absorption amount due to the minimizing bubble diameter.

➡ During the reactive crystallization with CO_2 microbubble injection, NaCl as by-product was generated because of the increase in Na^+ concentration by adding NaOH aqueous solution.